得なかった．こうした状態を考慮しmECT導入を決定，X年12月から家族の同意を得てパルス波治療器において週2回の頻度で計8回施行した．

mECTにより幻視，筋固縮ともかなりの改善をみた．嚥下機能に関しても経口薬摂取は可能となったが食事摂取は不可能で，経鼻栄養を終了できないなど改善効果は限定的であった．そのため，胃瘻増設や嚥下リハビリを検討せざるを得ず，最終的にはX+1年1月，他院へ転院した．

mECT(X年12月12日～X+1年1月5日)：

第1セッション：半年齢法に基づき35%で開始．

第1～3セッションまでは1回の通電で有効なけいれん得られず，2回通電．

第4～8セッションは1回の通電で有効なけいれんが得られた．

刺激容量：35～75%．

〔症例2〕67歳，女性．

診断：①妄想性障害，②悪性症候群．

主訴：発熱，筋固縮．

既往歴：特記すべき事項はない．

生活歴：高校卒業後はデパート店員として従事した．22歳で結婚し，挙児4名をもうけた．夫とは34歳時に離婚し以後は生活保護を受給し子を養育した．1年のうち1/3は寝込んで過ごし，1/3は忙しく家事をこなし，残りの1/3は穏やかに過ごしたため，子どもからは躁うつ病にみえていたという．40歳頃からは親戚の個人病院で事務職に従事した．その後も寝込むこともあったが親戚のため大目にみてもらっていた．

現病歴：Y－5年(62歳時)頃から近隣住民への被害妄想が出現した．この頃には「寝込む時期」は1年の2/3近くに延びていた．家族に連れられ近医を受診したところ妄想性障害と診断された．Y－3年にはほとんど自宅で寝込む生活となり，M病院に入院を勧められたが強く抵抗した．その割に入院後は非常に良く適応し短期間で退院した．しかし，退院後はまた寝込むだけの生活に戻り妄想も著しく再燃した．それでもY年1月まではデイサービスを利用するなどして生活できていたが，同年2月に妄想が再度活発化し同院に再入院した．Aripiprazolにより症状は改善し同年3月に退院したが，妄想は数日で急激に再燃し同院に再入院した．同薬での加療を継続されたが，筋固縮や体動減少が出現したことで悪性症候群を疑われ同薬は中止された．しかし症状は改善なく，神経内科に相談したところパーキンソニズムの可能性を指摘されpramipexoleを開始された．その後も薬剤調節を行われたが症状に変化なく，同年6月中旬には体温が39℃台まで上昇したため不明熱の精査目的に当科に転院した．

入院時現症：表情は変化に乏しく自発語はない．問いかけには返答できるが内容は要領を得ない．幻覚妄想，抑うつの存在は明らかでなかった．口唇，舌には振戦，流涎あり．両上肢に固縮，振戦，カタレプシーを認めた．

検査所見：

血液検査(Y年6月14日)：WBC 6,000/μl, CRP 2.54 mg/dl↑，Na 125 mmol/l↓，K 4.1 mmol/l, Cl 95 mmol/l↓，AST 60 U/l↑，ALT 94 U/l↑，CK 60 U/l, BUN 13 mg/dl, Cre 0.42 mg/dl, β-D-glucan 228.7 pg/ml(＞20)↑．

脳波：睡眠第2段階の記録．中心部～後頭部に14 Hz, 40～70 μVの紡錘波を認め左右差はない．突発波の混入は認めず．

頭部CT(Y年6月14日)：頭蓋内に明らかな異常所見はない．

頭部MRI(Y年7月2日)：側脳室下角の拡大あり，前頭葉や尾状核，被殻の萎縮が目立つ．

胸部～骨盤CT(Y年6月14日)：特記すべき所見はない．

脳SPECT：発熱のため未施行．

MIBG心筋シンチグラフィー：心筋の描出は良好で，DLBおよびPD関連疾患は否定的．

入院後経過(図2)：

転院時の画像診断では異常はない．中心静脈カテーテル挿入部周囲の発赤や，血液検査の結果等よりカテーテルからの真菌感染と診断し抗真菌薬を投与開始した．全身状態の改善を優先し抗精神病薬は中止した．

その後血液検査でβ-D-glucanは入院時から改善傾向となったが38℃前後の発熱は持続し，徐々に呼びかけへの反応は乏しくなり，自発的運動

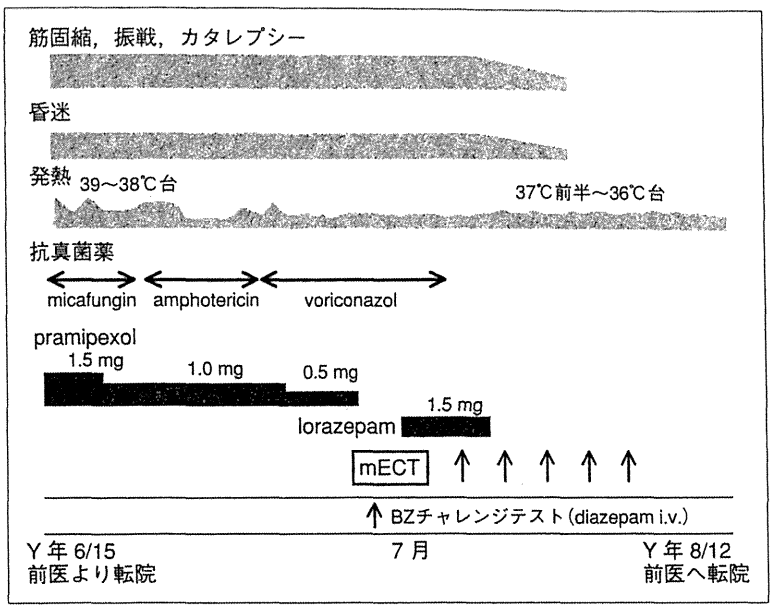

図2 症例2の入院後経過

はほぼ消失した．発熱の原因として真菌感染症も否定できないとしても，同時に緊張病症候群を呈している可能性を考えた．そのため，diazepamを経静脈的に投与したところ，発語が可能になるなど意欲面での改善が認められた．そのため，BZ系は有効と判断しlorazepamを投与開始したところ，発語は認められるようになったが疎通性は不良なままで，叫び声を上げるなどむしろ興奮が増強した．運動症状の改善は乏しく，さらには幻視を疑わせる訴えも出現するなど，症状改善は限定的で部分的な増悪も認めた．同年7月中旬には全身状態も安定し真菌感染症の治療も終了したが，上述のように緊張病症状は改善していないためmECTを導入すべきと判断し家族に説明し同意を得た．同年7月から導入し第2セッション後から疎通性，筋固縮とも改善傾向を認めた．第5セッションを終了した時点で会話内容も了解可能なほどに改善し，幻視や妄想も消失した．

その後本人と家族より症状が改善したため前医への転院が希望あり，同年8月に前医へ転院した．

mECT(Y年7月22～31日)：

第1セッション：半年齢法に基づき35%で開始．

第1セッションのみ1回の通電では有効なけいれん得られず2回通電．

第2～5セッションは1回の通電で有効なけいれんが得られた．

刺激容量：35～80%．

考　察

この2症例ではいずれも緊張病症候群を呈していると思われるが，それまでの病歴は大きく異なっている．

症例1は神経症状が数年間先行し，その後術後せん妄を契機として幻視を呈している．このときの幻視は誤認が中心であった．しかし，lorazepamを開始しL-DOPAを調節した後からは，「足元にサッカーボールが見える」など，特異的な幻視が出現している．小阪はパーキンソン病をL-DOPAで治療中に特徴的な幻視が出現した場合，DLBを疑うべきと主張している[4]．また，Nagahamaらは幻視を認める患者のSPECTで，左後頭葉腹側領域と両側縁上回，および角回の血流低下を報告している[5]．本症例では左の角回～縁上回周辺に血流低下があるが，血流低下の度合いは軽度であり幻視の原因との断定は困難と思われた．認知機能低下も認められているが，独居であったためどの時点から低下し始めたの

表1　レビー小体型認知症(DLB)診断基準改訂版

1：中心的特徴(診断に必須)
　認知症(正常な社会的・職業的機能に支障をきたすほどの進行性認知低下)
　早い時期には著明な，または持続性の記憶障害は必ずしも起こらなくてもよいが，通常は進行とともに明らかになる
　注意や実行機能や視空間能力のテストでの障害が特に目立つこともある
2：コア特徴(probable DLBの診断には2つ，possible DLBの診断には1つ)
　1)注意や明晰性の著明な変化を伴う認知の変動
　2)典型的には構築された具体的な繰り返される幻視
　3)特発性のパーキンソニズム
3：示唆的特徴(1つ以上のコア特徴があり，1つ以上の以下の特徴があれば，probable DLBの診断が可能．コア特徴がなくても，1つ以上の示唆的特徴があればpossible DLBの診断には十分．Probable DLBは示唆的特徴だけでは診断するべきではない)
　1)レム睡眠行動異常
　2)重篤な抗精神病薬への過敏性
　3)SPECTまたはPETで示される基底核でのドパミントランスポーターの取り込み低下
4：支持的特徴(普通はあるが，診断的特異性は証明されていない)
　繰り返す転倒や失神
　一過性の説明困難な意識消失
　重篤な自立神経障害：たとえば，起立性低血圧，尿失禁
　他の幻覚
　系統的な妄想
　抑うつ
　CT/MRIでの内側側頭葉の比較的保持
　SPECT/PETでの後頭葉低活性を伴う全般性低活性
　MIBG心筋シンチグラフィーでの取り込み低下
　脳波での側頭葉の一過性鋭波を伴う目立った徐波化
5：DLBの診断の可能性が乏しい
　局所性神経徴候や脳画像でみられる脳血管障害の存在時
　部分的あるいは全般的に臨床像を説明しうる他の身体疾患または脳疾患の存在時
　重篤な認知症の時期にはじめてパーキンソニズムが出現した場合

(文献[6]より引用)

かはっきりしない．診断はいわゆる「1年ルール」にのっとると，認知症を伴うパーキンソン病が考えられるが，臨床的にはこれをDLBと厳密に区別する意義は乏しいとされる[6]．本症例はDLB診断基準改訂版(表1)の，中心的特徴である進行性の認知機能低下に加え，中核的特徴である認知の変動，具体的な繰り返される幻視，特発性のパーキンソニズムの3つを認めたため，probable DLBと診断し，問題となる症状への対応を重視した．

症例2は，30代で出産した後は，1年間をうつ病期，軽躁期および寛解期でちょうど3等分しているかのようにみえた．こうした活動性の変化をみる限り躁うつ病圏の疾患が考えやすい．しかし，経年とともに「寝込む時期」，つまりうつ病相らしき時期が長引くようになり，初老期には被害関係妄想が出現している．この経過を振り返ると，古茶が遅発性緊張病について，症候学的特徴，病像の推移および経過について詳細にまとめている[7]が，患者は年に1回の周期で訪れる初期抑うつ期をどうにか乗り切っていたが，徐々に不安・焦燥期に移行してそれが困難になってしまったのではないであろうか．初回入院への強い抵抗は，その時期の強い不安・焦燥を表しているのであろう．その後連続して幻覚妄想期に至り，近所の人物を対象として妄想を抱いたため精神科初診時には妄想性障害との診断がなされ，抗精神病薬での治療が必要となったのであろう．

その後どちらの症例も(亜)昏迷，筋固縮，姿勢保持等の症状から緊張病症候群と判断された．身体疾患の治療後も改善しない発熱が持続することより，悪性緊張病の可能性も検討されたが，経過を通じて血圧や脈拍などはほぼ正常と自律

神経系は安定していた．

緊張病症候群の治療としては薬物療法としてはBZ系が第1選択薬とされる[1]．Rosebushらが緊張病症候群の急性期に対してlorazepamの効果を調べた試験によると，15例の急性期緊張病エピソードに対し同薬を1～2 mg投与したところ，2時間以内に12例(80％)で劇的に症状が消失したという[8]．本邦では長岡ら[9]，当科でも藤原ら[10]が緊張病症状を呈したDLBにBZ系を投与した症例について報告しているが，症例1のようにDLBである場合，認知機能への影響やBPSDの悪化等が危惧されるためBZ系の投与は慎重にならざるを得ない．今回の症例1では日中の睡眠覚醒リズムの障害を招いたため投与を断念した．しかし，当科の他の症例ではlorazepamが効果的と考えられたものもある．投与においては，単純にDLBに不利益と決めつけずベネフィットとリスクを慎重に検討することが重要であろう．

緊張病症候群に対するもう1つの治療としてmECTがあげられる．Finkは著書の中で，カタトニアの治療において薬物治療が失敗したらECTの出番であると述べている[2]．症例1はDLBと診断しているが，当科に転院直後から緊張病症候群を呈していることを考慮し，抗認知症薬ではなくBZ系での治療を優先し，その後にmECTを導入した．また，FinkはBZチャレンジテストについても述べている[2]が，症例2ではdiazepamへの反応は良好であったにもかかわらず，内服のlorazepamへの反応は期待したものとは異なり，興奮や幻視が前景に立つようになった．そのため，早急な症状の改善を期待し，mECTへ移行する方針とした．両症例とも，mECTを施行する際には，各セッションの波形の評価において，上田が述べているような評価項目を用いて評価し[11]，次回の刺激強度の決定の参考にした[12]．

その効果について振り返ると，両症例とも第1セッション当日の施行後から両上肢の筋固縮が改善し自発的運動も認められるなど，四肢の運動障害は著明な改善が認められた．昏迷からも脱し発語量も増えるなど意欲面での改善も認められた．解熱傾向となり誤嚥性肺炎も認めなくなった．精神症状に関しては幻視が減少し妄想や興奮も消失した．DLBの診断基準のうちの支持的特徴としてSPECTでの後頭葉の血流低下があるが[5,6]，これが幻視や視覚認知障害との関連が考えられている．矢野らの報告では，幻視，抑うつ，昏迷を呈したDLB症例で，mECT後にSPECTにおいて後頭葉の血流低下の改善を認めている[13]が，症例1でも類似した所見が認められる．前述のとおり症例1は血流低下の程度が軽度であり幻視の原因と断定するのは困難であるが，仮に，幻視の原因となるような局所的な血流低下をmECTにより改善できるとすれば，臨床症状およびSPECTの局所的な血流低下とも典型的な所見の場合，mECTの効果はある程度予測可能となるかもしれない．

おわりに

緊張病症候群を呈した2例を経験した．緊張病症候群に至るまでの経過は大きく異なっていたが，いずれも筋固縮，昏迷，発熱といった症状を認めた．治療反応性という観点においては，BZ(benzodiazepine)系に対する反応は異なっていたが，mECTには両者とも良好な反応を示した．レビー小体型認知症(dementia with Lewy bodies；DLB)と遅発緊張病という類似しながらも異なる部分もある疾患の2例であったが，実臨床においては緊張病症候群への治療を適切に行うことの重要性を再確認した．精神疾患で緊張病症状を認めた場合，操作的診断基準に従えば異なる診断とされる疾患においても緊張病症候群として新たな診断の亜型を提案することが可能ではないかと示唆される2症例であった．

文　献

1) 大久保善郎．カタトニア(緊張病)症候群の診断と治療．精神経誌 2010；112：396.
2) Fink M, Taylor MA. Catatonia : A Clinician's Guide to Diagnosis and Treatment. Cambridge : Cambridge University Press ; 2003.〔鈴木一正・訳．カタトニア．臨床医のための診断・治療ガイドライン．東京：星和書店；2007.〕
3) Taylor MA, Fink M. Catatonia in psychiatric classification : a home of its own. Am J Psychiatry 2003 ; 160 : 1233.
4) 小阪憲司．DLBの初期診断．Mod Physician 2006；

26：1869.
5) Nagahama Y, Okina Y, Suzuki N, Matsuda M. Neural correlates of psychotic symptoms in dementia with Lewy bodies. Brain 2010；133：557.
6) McKeith IG, Dickson DW, Lowe J, et al. Diagnosis and management of dementia with Lewy bodies：Third report of the DLB consortium. Neurology 2005；65：1863.
7) 古茶大樹．遅発緊張病について．日本生物学的精神医学会誌 2010；21：3.
8) Rosebuch PI, Hildebrand AM, Furlong BG, et al. Catatonic syndrome in a general psychiatric inpatient population：frequency, clinical presentation, and response to lorazepam. J Clin Psychiatry 1990；51：357.
9) 長岡研太郎，橋本　衛，大川愼吾．レビー小体病に生じた緊張病症候群にlorazepamが奏功した2症例．精神科治療学 2004；19：1259.
10) 藤原(大橋)愛子，久保達哉，杉本　流，ほか．自殺企図を呈し入院に至ったレビー小体型認知症の1例～その問題点と考察～．九神精医 2012；58：83.
11) 上田　諭．電気けいれん療法のエビデンス―施行方法が効果と安全性を決める―．老年精神医学雑誌 2013；24：471.
12) 上田　諭．発作脳波の有効性判定と1.5倍の刺激％上げ幅が必須―パルス波ECT施行の前提と倫理―．臨床精神医学 2013；42：421.
13) 矢野智宣，小野陽一，森　秀徳，ほか．m-ECTにより後頭葉の著明な血流改善を認めたDLBの1例．臨床精神医学 2006；35：1269.

*　　*　　*

Cellular Signalling 26 (2014) 2446–2459

Contents lists available at ScienceDirect

Cellular Signalling

journal homepage: www.elsevier.com/locate/cellsig

Heterozygous mutations in cyclic AMP phosphodiesterase-4D (PDE4D) and protein kinase A (PKA) provide new insights into the molecular pathology of acrodysostosis

Tadashi Kaname [a,1], Chang-Seok Ki [b,1], Norio Niikawa [c], George S. Baillie [d], Jonathan P. Day [e], Ken-ichi Yamamura [f], Tohru Ohta [g], Gen Nishimura [h], Nobuo Mastuura [i], Ok-Hwa Kim [j], Young Bae Sohn [k], Hyun Woo Kim [l], Sung Yoon Cho [m], Ah-Ra Ko [n], Jin Young Lee [n], Hyun Wook Kim [o], Sung Ho Ryu [o,p], Hwanseok Rhee [q], Kap-Seok Yang [q], Keehyoung Joo [r,s], Jooyoung Lee [r,s,t], Chi Hwa Kim [u], Kwang-Hyun Cho [v], Dongsan Kim [v], Kumiko Yanagi [a], Kenji Naritomi [a], Ko-ichiro Yoshiura [w], Tatsuro Kondoh [x], Eiji Nii [y], Hidefumi Tonoki [z], Miles D. Houslay [aa], Dong-Kyu Jin [m,*]

[a] Department of Medical Genetics, University of the Ryukyus Graduate School of Medicine, Okinawa, Japan
[b] Department of Laboratory Medicine and Genetics, Sungkyunkwan University School of Medicine, Seoul, Republic of Korea
[c] Health Sciences University of Hokkaido, Hokkaido, Japan
[d] Institute of Cardiovascular and Medical Sciences, College of Medical, Veterinary and Life Sciences, University of Glasgow, UK
[e] Department of Genetics, University of Cambridge, Cambridge, UK
[f] Division of Developmental Genetics, Institute of Resource Development and Analysis, Kumamoto University, Kumamoto, Japan
[g] Research Institute of Personalized Health Sciences, Health Sciences University of Hokkaido, Hokkaido, Japan
[h] Department of Pediatric Imaging, Tokyo Metropolitan Children's Medical Center, Tokyo, Japan
[i] Seitoku University, Chiba, Japan
[j] Department of Radiology, Gachon University Gil Medical Center, Incheon, Republic of Korea
[k] Department of Medical Genetics Ajou University Hospital, Ajou University School of Medicine, Suwon, Republic of Korea
[l] Department of Orthopedic Surgery, Yonsei University College of Medicine, Seoul, Republic of Korea
[m] Department of Pediatrics Samsung Medical Center, Sungkyunkwan University School of Medicine, Seoul, Republic of Korea
[n] Clinical Research Center, Samsung Biomedical Research Institute, Seoul, Republic of Korea
[o] Department of Life Sciences, Pohang University of Science and Technology, Pohang, Republic of Korea
[p] Division of Integrative Biosciences and Biotechnology and School of Interdisciplinary Bioscience and Bioengineering, Pohang University of Science and Technology, Pohang, Republic of Korea
[q] Macrogen Inc., Seoul, Republic of Korea
[r] Center for In Silico Protein Science, Korea Institute for Advanced Study, Republic of Korea
[s] Center for Advanced Computation, Korea Institute for Advanced Study, Republic of Korea
[t] School of Computational Sciences, Korea Institute for Advanced Study, Republic of Korea
[u] Mogam Biotechnology Research Institute, Yongin, Republic of Korea
[v] Department of Bio and Brain Engineering, Korea Advanced Institute of Science and Technology (KAIST), Republic of Korea
[w] Department of Human Genetics, Nagasaki University Graduate School of Biomedical Sciences, Nagasaki, Japan
[x] Division of Developmental Disabilities, The Misakaenosono Mutsumi Developmental, Medical and Welfare Center, Isahaya, Japan
[y] Department of Orthopaedic Surgery, Mie Prefectural Kusanomi Rehabilitation Center, Tsu, Japan
[z] Section of Clinical Genetics, Department of Pediatrics, Tenshi Hospital, Sapporo, Japan
[aa] Institute of Pharmaceutical Science, King's College, London, UK

ARTICLE INFO

Article history:
Received 14 June 2014
Received in revised form 16 July 2014
Accepted 16 July 2014
Available online 24 July 2014

Keywords:
Acrodysostosis

ABSTRACT

Acrodysostosis without hormone resistance is a rare skeletal disorder characterized by brachydactyly, nasal hypoplasia, mental retardation and occasionally developmental delay. Recently, loss-of-function mutations in the gene encoding cAMP-hydrolyzing phosphodiesterase-4D (*PDE4D*) have been reported to cause this rare condition but the pathomechanism has not been fully elucidated. To understand the pathogenetic mechanism of *PDE4D* mutations, we conducted 3D modeling studies to predict changes in the binding efficacy of cAMP to the catalytic pocket in PDE4D mutants. Our results indicated diminished enzyme activity in the two mutants we analyzed (Gly673Asp and Ile678Thr; based on PDE4D4 residue numbering). Ectopic expression of PDE4D mutants in HEK293 cells demonstrated this reduction in activity, which was identified by increased cAMP levels. However,

* Corresponding author at: Department of Pediatrics, Samsung Medical Center, Sungkyunkwan University School of Medicine, Samsung Medical Center, 50 Irwon-dong, Gangnam-gu, Seoul 135-710, Republic of Korea. Tel.: +82 2 3410 3525; fax: +82 2 3410 0043.
E-mail address: jindk@skku.edu (D.-K. Jin).
[1] The first two authors (T.K. and C.-S.K.) contributed equally to this work.

http://dx.doi.org/10.1016/j.cellsig.2014.07.025
0898-6568/

PDE4D
cAMP
Knok out rat

the cells from an acrodysostosis patient showed low cAMP accumulation, which resulted in a decrease in the phosphorylated cAMP Response Element-Binding Protein (pCREB)/CREB ratio. The reason for this discrepancy was due to a compensatory increase in expression levels of PDE4A and PDE4B isoforms, which accounted for the paradoxical decrease in cAMP levels in the patient cells expressing mutant isoforms with a lowered PDE4D activity. Skeletal radiographs of 10-week-old knockout (KO) rats showed that the distal part of the forelimb was shorter than in wild-type (WT) rats and that all the metacarpals and phalanges were also shorter in KO, as the name acrodysostosis implies. Like the G-protein α-stimulatory subunit and PRKAR1A, PDE4D critically regulates the cAMP signal transduction pathway and influences bone formation in a way that activity-compromising *PDE4D* mutations can result in skeletal dysplasia. We propose that specific inhibitory PDE4D mutations can lead to the molecular pathology of acrodysostosis without hormone resistance but that the pathological phenotype may well be dependent on an over-compensatory induction of other PDE4 isoforms that can be expected to be targeted to different signaling complexes and exert distinct effects on compartmentalized cAMP signaling.

1. Introduction

Acrodysostosis is a group of rare skeletal disorders characterized by brachydactyly, nasal hypoplasia, mental retardation, and occasionally developmental delay [1]. Progressive growth failure, short stature, and severe mid-face hypoplasia with skull deformity are common features of this disorder [1,2]. Acrodysostosis is phenotypically heterogeneous, and at least two groups are recognized: acrodysostosis with hormone resistance (OMIM #101800) and without hormone resistance (OMIM #614613). Acrodysostosis has attracted attention because the disorder shares common skeletal changes with Albright's hereditary osteodystrophy (AHO) or pseudohypoparathyroidism type 1a (PHP-1a). However, neither the biochemical impairment of the activity of G-protein α-stimulatory subunit (GNAS), which activates adenylyl cyclase and cAMP production [3], nor the genetic mutation of GNAS associated with PHP-1a, have been observed in individuals with acrodysostosis [1,4]. Recently, 3 patients with acrodysostosis with hormone resistance were identified to harbor the same nonsense mutation in the *PRKAR1A* gene [5]. The *PRKAR1A* gene encodes the cAMP-binding regulatory subunit of protein kinase A (PKA) that, together with an exchange protein activated by cAMP (Epac) [6], functions as a key intracellular signal transducer in Gsα-cAMP signaling.

Cyclic AMP levels are dynamically regulated not only by the activation of adenylyl cyclase but also by the inhibition of cAMP phosphodiesterases (PDEs), which provide the sole route for inactivation of this second messenger in the cells [7,8]. Of the PDE superfamily, selective inhibitors of the cAMP-specific phosphodiesterase-4 (PDE4) family have been shown to have profound anti-inflammatory actions [9–11] and have demonstrable therapeutic utility in both COPD (roflumilast) [12–14] and psoriatic arthritis (apremilast) [15,16].

Four genes encode the PDE4 family (PDE4A, PDE4B, PDE4C, PDE4D) with alternative splicing generating >20 isoforms [7,17]. A key functional consequence of this diversity is that various signaling scaffold and other proteins are able to sequester specific PDE4 isoforms [7, 18–20]. This tethering leads to the spatial localization of individual types of PDE4 isoforms which act to underpin compartmentalized cAMP signaling by shaping gradients of cAMP in distinct intracellular locales [7]. This ability confers non-redundant functional roles on specific PDE4 isoforms as uncovered using dominant negative [21–24] and siRNA (small interfering RNA)-mediated knockdown [25] approaches. In this, PDE4A1 provides the paradigm for PDE targeting [26–28], while PDE4D5 provides the paradigm for a particular PDE isoform being able to regulate a specific cellular function through targeting [29].

Individual PDE4 isoforms have distinct, intronic promoters that confer cell-type specific patterns of expression. Although little is known about these it has been shown that sustained changes in cAMP levels can alter expression levels of particular PDE4 isoforms, some of which have CRE loci that allows for their regulation by PKA phosphorylated CREB [30–33].

PDE4 isoforms are sub-categorized into long forms with UCR1 and UCR2 regulatory regions; short forms lacking UCR1 and super short forms lacking UCR1 but with a truncated UCR2 [7,34]. When cAMP levels are elevated in cells, the long PDE4 isoforms play a pivotal and exclusive role in determining both the magnitude and duration of this response through their activation through phosphorylation by cAMP-dependent protein kinase A (PKA) [35–43].

PDE4 long isoforms thus play a key role in underpinning both the cellular desensitization to cAMP as well as determining the compartmentalization of cAMP signaling. As such, changes in their activity, localization, post-translational regulation and the complement of different isoforms expressed in a particular cell are set to have profound physiological consequences [7].

Here, we present data collected using 3 approaches. First, in a mutation study, we identified 7 patients with acrodysostosis without hormonal resistance, linking the disease with the gene for cAMP-specific phosphodiesterase 4D (PDE4D). Second, in functional studies, we analyzed the 3D structure of PDE4D mutants and measured the activity of PDE4D mutants transfected into heterologous cells; we also colocalized PDE4D and β-arrestin using confocal microscopy and determined PDE4 activity and isoform expression in patient cells. Third, we generated PDE4D knockout (KO) rats and demonstrated that PDE4D loss results in the skeletal dysplasia phenotype observed in acrodysostosis. This work opens up a new horizon in the pathogenesis of acrodysostosis by showing that acrodysostosis without hormone resistance can be caused by alterations in cAMP degradation by PDE4D [7] and results in skeletal dysplasia.

2. Methods

2.1. Patient enrolment

Seven patients diagnosed as acrodysostosis without hormone resistance were included in the study. The patients represent all of the available patients diagnosed at the time of the study in Korea and Japan. Diagnosis was made by the typical X-ray features and the confirmation of the absence of the hormone resistance. The details of clinical features including hormone profiles are described in Table 1. One patient diagnosed as acrodysostosis without hormone resistance, who harbor the *PRKAR1A* mutation was included in the functional study for comparison.

The clinical features of 1 Korean (patient 2) and 3 Japanese patients (patients 4, 5 and 7) were described previously [44–46]. The mother of the Japanese siblings (patients 4 and 5) was reported to be affected mildly. For the other patients, clinical features are summarized in Table 1. Informed consent was obtained from the parents of all patients and this study was approved by the Institutional Review Board.

2.2. DNA study

Exome sequencing was performed on 2 Korean patients and 2 Japanese siblings with acrodysostosis (4 patients in 3 families), as well

Table 1
Clinical and laboratory findings of patients
Identifying mutations in acrodysostosis patients. Exomes were sequenced in 8 patients with acrodysostosis. We found that patient 8 had a de novo p.Arg368* mutation in *PRKAR1A*. When we compared the gene lists from patients other than patient 8, *PDE4D* was identified as the only gene they all shared.

	Patient 1	Patient 2	Patient 3	Patient 4	Patient 5	Patient 6	Patient 7	Patient 8	Reference range
Previous reports	Unpublished	Ref 9	Unpublished	Ref 8	Ref 8	Unpublished	Ref 10	Unpublished	
Gene	*PDE4D*	*PDE4D*	*PDE4D*	*PDE4D*	*PDE4D*	*PDE4D*	*PDE4D*	*PRKAR1A*	
Mutation	c.2033 T > C (p.I678T)	c.2018G > A (p.G673D)	c.2033 T > C (p.I678T)	c.683A > C (p.Q228P)	c.683A > C (p.Q228P)	c.689 T > C (p.L230S)	c.1759A > G (p.T587A)	c.1101C > T (p.R368X)	
Clinical findings									
GA (wk)/ Bwt (kg)	40/2.8	40/2.9	41/2.3	40/2.22	40/2.35	41/2.5	38/2.3	37 + 4/2.08	
Sex/age (y)	F/17 y	M/17 y	M/4 y 11 m	F/39 y	M/37 y	M/10 y 5m	F/8 y 5 m	M/3 y 9 m	
Height (cm)/ SD	144.7/−3.1	155/−2.8	98.8/−1.4	149/-2.1	135/-5.9	137.2/-0.9	131.6/-0.2	95.6/−1.7	
Weight (kg)/ SD	54/−0.1	57/−0.7	15/-1.6	54.3/0	42.3/-2.2	37.2/-0.6	31/0.2	15.7/−0.6	
Short nose with flat nasal bridge	+ (Nose vestigial)	+ (Nose vestigial)	+	+ (Nose vestigial)	+ (Nose vestigial)	+ (Nose vestigial)	+ (Nose vestigial)	+	
Prominent forehead	+	+	+	+	+	+	+	+	
Iris color at infancy*	Light brown	Black	Gray	Gray	Gray	Gray	Gray > brown	Gray	
Mental retardation	Mild	Severe	Severe	Severe	Severe	Mild to Severe	Severe	Mild	
Developmental milestone	Delayed	Delayed	Delayed	Delayed	Delayed	Delayed	Delayed	Normal	
Radiologic findings									
Peripheral skeletal dysplasia	Severe	Severe	Severe	Severe	Severe	Severe	Severe	Mild	
Nasomaxillary hypoplasia	Severe	Severe	Severe	Severe	Severe	Severe	Severe	Mild	
Brachydactyly	Severe	Severe	Severe	Severe	Severe	Severe	Severe	Mild	
Advanced bone age	Yes	Yes	Yes	Yes	Yes	Yes	Yes	Yes	
Laboratory findings									
Hormonal resistance	No	No	No	No	No	No	No	Yes	
PTH/Ca/P	34/9.8/3	9/4.1	NA/10.2/4.5	64.4/9.4/3.2	61.7/9.3/3.4	41/9.6/4.4	NA/9.8/5.3	56/9.5/5.0	PTH: 11–62 pg/ml Ca: 8.4–10.2 mg/dl P: 2.5–4.5 mg/dl
25-vit. D	15.29	NA	NA	NA	NA	NA	NA	34.52	8–51.9 mg/dl
fT4/TSH	1.54/2.25	1.17/0.91	1.5/1.54	1.25/1.25	1.26/0.41	1.6/1.79	1.15/NA	0.98/67.51	fT4: 0.89–1.8 ng/dl TSH: 0.35–5.5 ulU/ml
hGH	0.05	NA	NA	NA	NA	NA	NA	0.82	0–4.7 ng/ml
IGF-1	210.8	272.3	112.6	NA	NA	NA	NA	152.6	49–642 ng/ml
LH/FSH	3.1/6.3	5.5/3.5	NA	NA	NA	NA	0.1>/1.8	1.2/1.5	LH: 0–10.6 ulU/ml FSH: 0.1–9 ulU/ml
ACTH	9.9	NA	NA	NA	NA	NA	88.3	34.8	0–60 pg/ml
Estradiol	39	2.95	NA	NA	NA	0.11	NA	<0.01	Estradiol: 10–441 pg/ml
Testosterone**									Testosterone: 2.79–8.76 ng/ml

* Reference cDNA sequence: NM_001104631.

as on the family members of the Korean patients (both parents and a brother of patient 1; mother and a sister of patient 2; and both parents of patient 8). After identifying the causative gene, exomes of 3 unrelated Japanese patients were also analyzed.

2.2.1. Exome sequencing

2.2.1.1. Library construction. Each sample that was sequenced was prepared according to Illumina protocols. Briefly, 1 μg of genomic DNA was fragmented by nebulization, the fragmented DNA was repaired, an 'A' was ligated to the 3′ end of fragments, Illumina adapters were then ligated to the fragments, and the samples were size selected, aiming for products of 350–400 base pairs. The size-selected products were amplified using PCR, and each final product was validated using Agilent Bioanalyzer. Before first hybridization, multiple libraries with distinct indices were combined into a single pool and then enrichment. The pooled DNA libraries were mixed with the "capture" probes against the targeted regions and incubated for the recommended hybridization time, which ensured that the targeted regions bound completely to the capture probes. Streptavidin beads were used to capture the probes bound to the targeted regions and the beads were washed thrice to remove non-specifically bound DNA. The enriched library was then eluted from the beads and prepared for a second hybridization. The DNA library obtained from the first elution was mixed with the capture probes against the target regions, and the second hybridization ensured that the targeted regions were enriched further. Streptavidin beads were used again to capture the probes containing the targeted regions and the beads were washed thrice to eliminate non-specifically bound DNA. The library thus enriched was eluted from the beads and prepared for sequencing. PCR was used to amplify the enriched DNA library for sequencing. PCR was performed using the same PCR primer cocktail used in TruSeq DNA Sample Preparation. Axeq Technologies conducted quality-control analysis on the sample library and quantified the DNA library templates.

2.2.1.2. Clustering and sequencing. Illumina used a unique "bridged" amplification reaction that occurs on the surface of the flow cell. A flow cell containing millions of unique clusters was loaded into HiSeq 2000 for automated cycles of extension and imaging.

2.2.1.3. Extension and imaging. Solexa's Sequencing-by-Synthesis used 4 proprietary nucleotides possessing reversible fluorophore and termination properties. Each sequencing cycle occurred in the presence of all 4 nucleotides, leading to a higher accuracy than with methods where a single nucleotide at a time is present in the reaction mix. This cycle was repeated, one base at a time, generating a series of images, each representing a single base extension at a specific cluster.

2.2.1.4. Sequence analysis. Paired-end sequences produced by HiSeq 2000 were mapped to the human genome, where the reference sequence was the UCSC assembly hg19 (NCBI build 37), without unordered sequences and alternate haplotypes; the mapping program used was BWA (version 0.5.9rc1). Uniquely mapped reads were only included for the latter steps. After generating a consensus sequence by creating a pileup file from the BAM file, a variant-calling process was run using SAM tools (version 0.1.12a), at which stage candidate SNPs and short indels were detected at nucleotide resolution. These variants were then annotated using ANNOVAR (version 2011Jun18) based on functional predictions, including SIFT and PolyPhen, to filter SNPs from the dbSNP for versions of 131 and 132, and to search SNPs from the 1000 Genomes project. Finally, in-house scripts and open programs were used to estimate various numbers obtained from all stages.

For consistency, the PDE4D residue numbering that we adopt here is based on the reference PDE4D4 isoform (GenBank accession No. NP_001098101) because the Leiden Open Variation Database (LOVD) of human Mendelian genetic variation uses human PDE4D4 (NP_001098101) as the reference sequence.

2.2.2. Sanger sequencing

Genomic DNA was extracted from peripheral blood leukocytes using Wizard Genomic DNA Purification kit, following the manufacturer's instructions (Promega). *PDE4D* exons and their flanking introns were amplified using primer sets we designed (available upon request). PCR was performed using a thermal cycler (model 9700, Applied Biosystems) as follows: 32 cycles of denaturation at 94 °C for 30 s, annealing at 60 °C for 30 s, and extension at 72 °C for 30 s. After treating the amplicon (5 μL) with 10 U of shrimp alkaline phosphatase and 2 U of exonuclease I (USB Corporation), direct sequencing was performed using a BigDye Terminator Cycle Sequencing Ready Reaction kit (Applied Biosystems) on an ABI Prism 3130xl genetic analyzer (Applied Biosystems). Novel *PDE4D* variants were confirmed on more than 2000 ethnicity-matched control chromosomes by sequencing. To describe sequence variations, we followed the guidelines of the Human Genome Nomenclature Committee (HGVS); the 'A' of the ATG translation start site was numbered +1 in DNA sequences and the first methionine was numbered +1 in protein sequences.

2.3. Functional studies

The disease-associated mutants are denoted as per PDE4D4 as the LOVD of human Mendelian genetic variation using human PDE4D4 (NP_001098101) as the reference sequence. This particular isoform is not widely expressed and is found predominantly in the brain [47]. We, have thus made and functionally characterized these mutations in the commonly expressed PDE4D5 isoform [47].

To predict the structural change in PDE4D mutations, molecular modeling and docking simulation of wild-type (WT) and mutant PDE4D were conducted, and we tested whether overexpression of recombinant WT or mutant PDE4D5 proteins affects the intracellular cAMP levels in HEK293 cells after treating with the adenylyl cyclase activator, forskolin.

Next, we measured the cAMP-hydrolyzing activity of the PDE4D mutant in Epstein–Barr virus (EBV)-transformed lymphocytes from patient 8 (with *PRKAR1A* p.R368* mutation) and patient 6 (with *PDE4D* p.L230S mutation), and we determined the phosphorylated Cyclic AMP Response Element-Binding Protein (pCREB):CREB ratio in the patient cells by Western blotting. We also measured total PDE and PDE4-specific activity to determine whether *PDE4D* mutations affect cAMP hydrolysis in the EBV-immortalized lymphocytes from the patients and control subjects. We determined the total cAMP-hydrolyzing activity in the presence or absence of the pan-PDE inhibitor IBMX, which inhibits all cAMP-hydrolyzing PDEs except PDE8 [8]. We also conducted these assays in the presence of the PDE4-specific inhibitor rolipram [8–11] to estimate the PDE4 fraction of total PDE activity. Lastly, we measured the expression of PDE4 and its isoforms in the patient cells and control cells.

2.3.1. Molecular modeling and docking simulation of wild-type and mutated PDE4D

We built 3D structural models for the catalytic domain of the PDE4D wild-type (WT) and its 2 mutants (p.Gly673Asp and p.Ile678Thr; based on PDE4D4). In PDB, several X-ray structures of PDE4D are available, and their overall structures are similar to each other and display a conserved shape for the cAMP-binding pocket. For 3D modeling, we employed a recently proposed high-accuracy template-based modeling method [48]. This method based on global optimization was shown to be successful in recent CASP7 and CASP8 protein-structure prediction experiments [49–51]. A total of 9 templates were used as core templates (3G4G, 1ZKN, 1OYN, 1ROR, 3LY2, 3G4I, 2QYK, 3DYN, and 2OUR), and 4 additional templates were used in a combinatorial manner (2H44, 1TBF, 3JWQ, and 3ITU) to consider 16 possible template combinations. The

final 3D model of each target sequence was selected from among 1600 candidate models by assessing their quality and comparing their structure with the X-ray structure of WT PDE4D (3G4I). The final models were all similar to 3G4I, with backbone RMSDs being approximately 0.4 Å (0.4×10^{-10} m). To estimate the binding affinity between the protein 3D models and cAMP, we performed docking simulations by using AutoDock Vina [52], a new and improved version of AutoDock. We performed flexible docking by considering these 14 flexible side-chains around the cAMP-binding pocket of PDE4D4: D503, D620, Q671, N623, G673 (D673 for p.Gly673Asp), I678 (T678 for p.Ile678Thr), Y461, H462, H466, H502, M575, L621, I638, and F642. A total of 30 exhaustive docking simulations were performed for each protein model.

2.3.2. CREB phosphorylation assay

For Western blotting analysis of phosphorylated-CREB levels in cells, EBV-transformed lymphocytes or HEK293 cells were harvested, washed with phosphate buffered saline (PBS), and lysed in RIPA buffer. Proteins were quantified using the BCA assay (Pierce). Equal amounts of whole cell lysates were separated using SDS-polyacrylamide gel electrophoresis (SDS-PAGE) and transferred to nitrocellulose membranes. Western blotting was performed using antibodies against CREB phosphorylated at Ser133 (pCREB) and total CREB (Cell Signaling Technology). Blots were developed using a peroxidase-conjugated secondary antibody and ECL Plus Western Blotting Detection System (Amersham™).

2.3.3. Quantification of cAMP

The cAMP-measuring kit was purchased from R&D Systems (Abingdon); cellular cAMP concentrations were measured using the competitive-binding technique, according to the manufacturer's instructions.

2.4. Generation of PDE4D knockout rats

The PDE4D knockout (KO) rats were generated and provided by Transposagen Biopharmaceuticals (Lexington, KY). $Pde4d^{Tn(sb\text{-}T2/Bart3)2.285Mcwi}$ on an F344 background was produced by a single-gene trap method based on the Sleeping Beauty transposable element [53]. After confirming trap-vector insertion in the 1st intron of *PDE4D*, rats homozygous for the PDE4D-targeted KO mutation were mated and pups were used for further analyses.

3. Results

3.1. Patient profiles and mutations

Seven patients diagnosed as acrodysostosis without hormone resistance were included in the study. The clinical and molecular characteristics of the patients are summarized in Table 1, and detailed mutation profiles and radiographs of patients are presented in Fig. 1A–J. The disease-associated mutants are denoted as per PDE4D4 as the LOVD of human Mendelian genetic variation uses human PDE4D4 (NP_001098101) as the reference sequence [47].

3.2. Three dimensional structure analysis of PDE4D mutants

Analyzing the 3D structure of the PDE4D mutants predicted changes in the binding efficacy of cAMP to the catalytic pocket in PDE4D mutants, indicating diminished enzymatic activity in the mutants (Table 2 and Fig. 2).

Cartoon figures of protein backbone structures (WT, p.Gly673Asp, and p.Ile678Thr; based on PDE4D4) with bound cAMP are shown in superposition in Fig. 2. The 3D models show few structural differences between WT and the 2 mutants in their backbones and side-chains, except for the mutated residues. The 2 mutated residues (p.Gly673Asp and p.Ile678Thr), which are positioned at the right-hand side of the cAMP-binding pocket, are represented by purple stick figures in Fig. 2B. Table 2 shows the average lowest binding affinity in a docking simulation between PDE4D and its substrate, cAMP. We observed that the WT protein was slightly more stable with cAMP, by approximately 0.17 kcal/mol, than the 2 mutants. This is because the WT and mutants have the same conserved binding residues (D503, D620, and Q671) around the cAMP-binding site, according to the Uniprot annotation; consequently, the binding conformations that correspond to the lowest binding energy are nearly identical, with only small variations in side-chain conformation around cAMP (Fig. 2B). The lowest binding energy and the number of successful bindings of each protein model are shown in Table 2. A successful binding corresponds to the formation of appropriate hydrogen bonds between cAMP and the binding residues of each protein (Fig. 2B). The standard deviation was calculated from 30 independent docking simulations. For WT PDE4D, all 30 simulations resulted in the same successful docking conformation that is shown in Fig. 2B. By contrast, the lowest energy binding conformations of the 2 mutants were found only 4 and 9 times out of 30 simulations (Fig. 2B), implying that the mutated residues entropically deter the binding of cAMP to the catalytic pocket and possibly affect enzymatic activity. The multiple sequence alignment used for 3D modeling showed that G673 is conserved and I678 is either conserved or substituted by a similar hydrophobic residue such as Val.

The Gly673Asp mutation results in the small neutral Gly residue in the WT protein being exchanged for a bulky negatively charged Asp residue. This Asp residue in the mutant could potentially interact with the –OH of cAMP and either block or inhibit cAMP entry into the binding pocket, thereby preventing efficient catalysis.

The Ile678Thr mutation exchanges a hydrophobic Ile residue for a hydrophilic Thr residue. Hydrophobic residues generally shield hydrogen bonds that form between the ligand and the protein in the catalytic pocket by providing a protective hydrophobic cap. Therefore, ablation of this hydrophobicity by the replacement with hydrophilic Thr likely interferes with critical internal hydrogen bonds between the protein and cAMP, and could therefore attenuate effective catalysis.

3.3. Functional studies on PDE4D mutants

PDE4D encodes a series of isoforms generated through the use of alternative promoters and alternative mRNA splicing. These isoforms are characterized by unique N-terminal regions that are invariably employed to target them to specific signaling complexes in cells, thereby conferring the unique functionality of the PDE4D isoforms [7,19]. The reference PDE4D isoform, PDE4D4 isoform is not widely expressed and is found predominantly in the brain [47]. We, have thus made and functionally characterized these mutations in the commonly expressed PDE4D5 isoform [47].

We assessed the functional activity of the Gsα-cAMP-PKA signal transduction pathway in the cells by measuring cAMP hydrolysis and the phosphorylation status of CREB, which is a pivotal target for PKA action. PDE4D5 is a common PDE4D long isoform responsible for desensitizing cAMP signals that arise from Gs-coupled cell-surface receptors [54]. We analyzed whether overexpressing recombinant WT or mutant PDE4D5 proteins affects intracellular cAMP levels in HEK293 cells treated with forskolin, which activates adenylyl cyclase. Whereas overexpressing WT PDE4D5 markedly lowered forskolin-stimulated cAMP levels, overexpressing Q228P-, G673D-, and I678T-PDE4D5 mutants at similar expression levels did not (Fig. 3A).

Next, we measured the cAMP-hydrolyzing activity of PDE4D mutants in EBV-transformed lymphocytes from patient 8 (with *PRKAR1A* p.R368X mutation) and patient 6 (with *PDE4D* p.L230S mutation). The cAMP level in the cells from patient 6 was significantly lower at 30 min after treatment with forskolin when compared to the cells from the control subject ($P = 0.02$, Fig. 3B).

Western blotting demonstrated that the pCREB to CREB ratio was significantly decreased in the cells from both patients 6 and 8 when

compared with the cells from the control subject (Fig. 3C and D): the basal level of pCREB in EBV-transformed cells from both patients was lower than in the control cells (Fig. 3C), and, after a 30-min treatment with forskolin, lower levels of pCREB were detected in the cells from the patients than in control (Fig. 3D). All cells had similar total CREB levels (Fig. 3B and D).

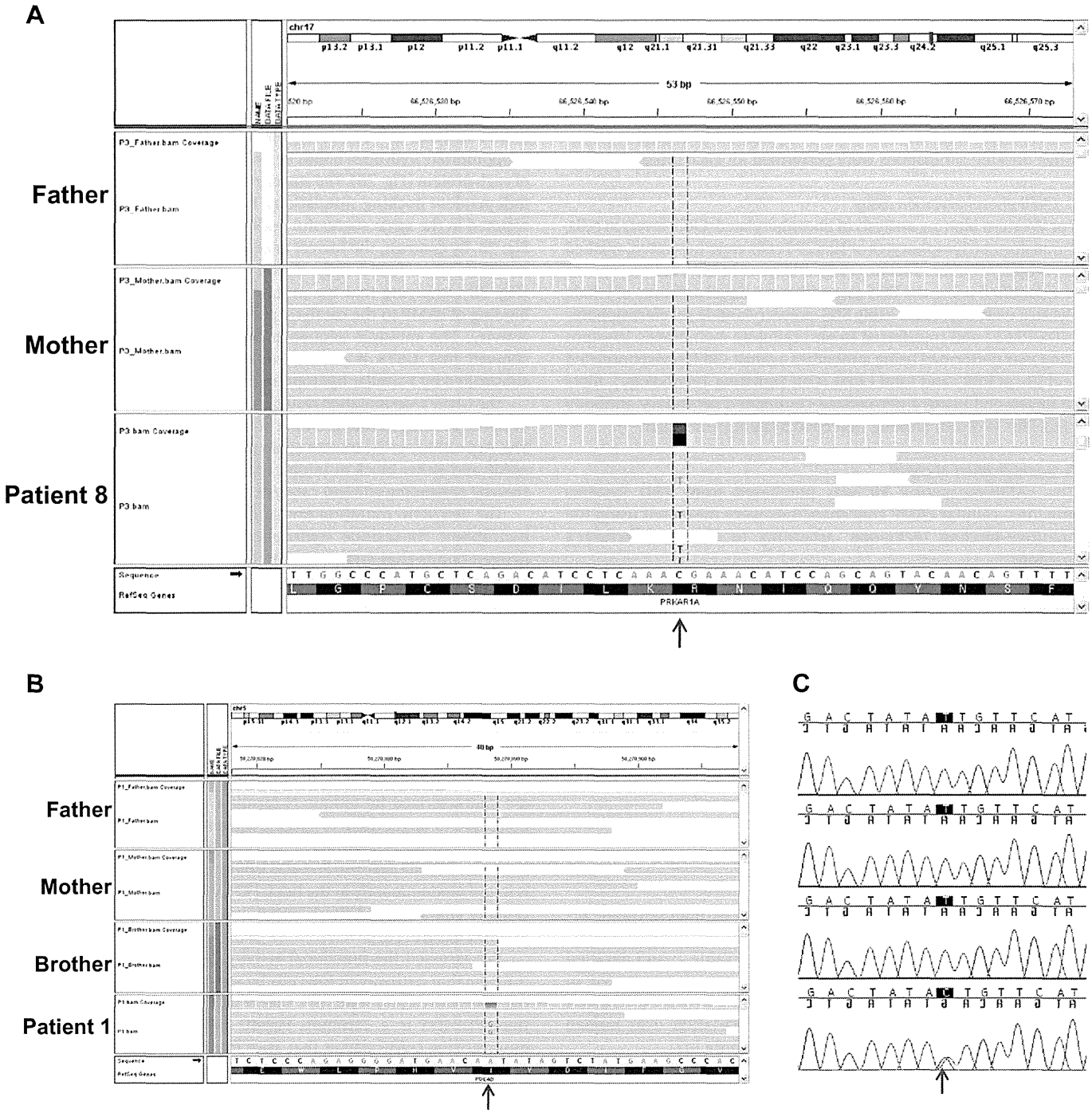

Fig. 1. Identification and confirmation of *PRKAR1A* and *PDE4D* mutations. A; The IGV browser view of the *PRKAR1A* gene region from the exome sequencing data shows that patient 8 (bottom panel) has the c.1101C > T (p.Arg368X) mutation in the *PRKAR1A* gene (arrow), but the father (top panel) and mother (middle panel) have the WT sequence. B; The IGV browser view of the *PDE4D* gene region from the exome sequencing data shows that patient 1 (bottom panel) has the c.2033 T > C (p.Ile678Thr) mutation in the *PDE4D* gene (arrow), but the father (top panel), mother (upper middle panel), and brother (lower middle panel) have the WT sequence. C; Sanger sequencing confirmed that patient 1 has a heterozygous mutation (c.2033 T > C; p.Ile678Thr) in the *PDE4D* gene (arrow), whereas the other family members have WT sequences. D; The IGV browser view of the *PED4D* gene region from the exome sequencing data shows that patient 2 (bottom panel) has the c.2018G > A (p.Gly673Asp) mutation in the *PDE4D* gene (arrow), but the mother (top panel) and sister (middle panel) have the WT sequence. E; Sanger sequencing confirmed that patient 2 has a heterozygous mutation (c.2018G > A; p.Gly673Asp) in the *PDE4D* gene (arrow), whereas the other family members have WT sequences. F; A comparison of the protein sequences of human, chimpanzee, orangutan, dog, mouse, and zebra fish orthologs of PDE4D shows that p.Gly673 and p.Ile678 are highly conserved residues. G; The IGV browser view of the *PED4D* gene region from the exome sequencing data shows that patient 4 (upper panel) and patient 5 (lower panel) have the c.683A > C (p.Gln228Pro) mutation in the *PDE4D* gene (arrow). H; Sanger sequencing confirmed that patients 4 and 5 have a heterozygous mutation (c.683A > C; p.Gln228Pro) in the PDE4D gene (arrow). I; Schematic diagram and Sanger sequencing of 3 mutations detected in the *PDE4D* genes in patients 6, 7, and 3. Mutations are indicated on a PDE4D protein structure with conserved domains. P: phosphorylation sites. UCR: upstream conserved region. J; X-ray views of hands and feet of patients 1, 2, and 8 revealing typical characteristics of acrodysostosis: shortening of the metacarpals, metatarsals, phalanges, and cone-shaped epiphyses. Patients 1 and 2 showed more severe bony abnormalities than patient 8.

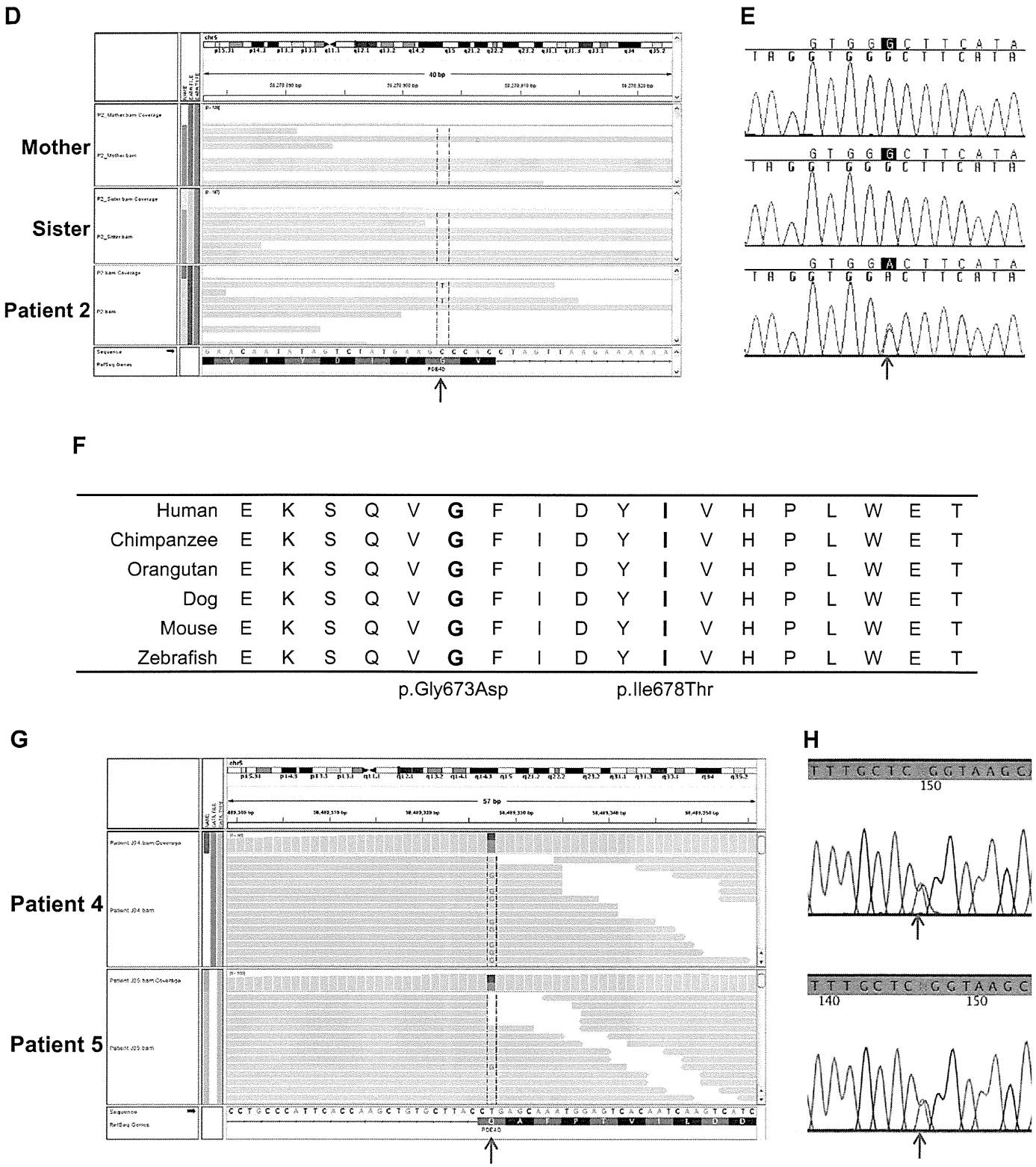

Fig. 1 (*continued*).

3.4. PDE4-specific activity

We investigated the activity of the PDE4 mutants found in patients to determine whether the mutations affect the cAMP-hydrolyzing capability of the enzyme. Five distinct PDE4D mutant constructs (Q164P, L166S, T523A, G609D, and I614T; based on PDE4D5 [47], Table 3) were overexpressed in HEK293 cells and lysates containing equal amounts of WT and mutant PDE4D proteins were used to assess the proteins' ability to hydrolyze cAMP (Fig. 3A). Relative to WT PDE4D, all the PDE4D mutants exhibited markedly diminished cAMP-hydrolyzing activity. Therefore, inserting the PDE4 gene mutations found in patients with acrodysostosis without hormone resistance into PDE4D4 severely compromised the catalytic activity of PDE4D4.

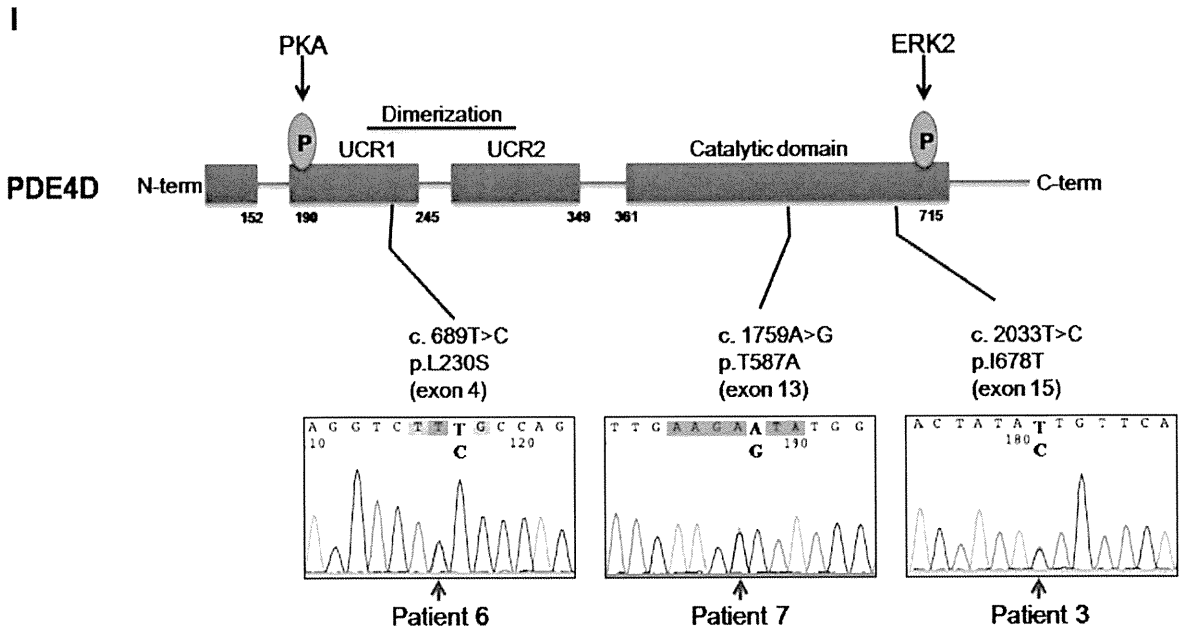

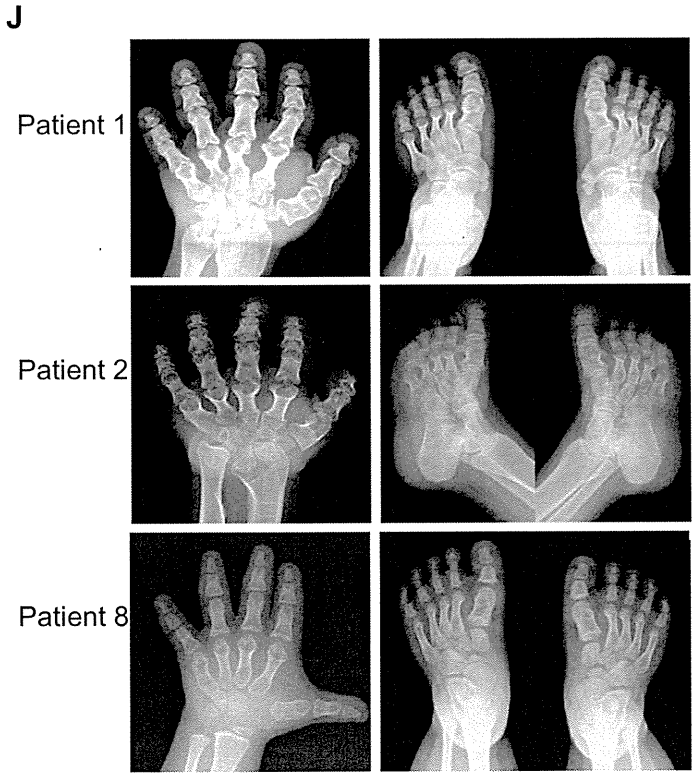

Fig. 1 (*continued*).

Next, we measured the cAMP PDE activity in EBV-immortalized lymphocytes from control subjects and patients. We determined the total cAMP-hydrolyzing activity in the presence or absence of the pan-PDE inhibitor IBMX, which inhibits all cAMP-hydrolyzing PDEs except PDE8 [8]. We also conducted these assays in the presence of the PDE4-specific inhibitor Rolipram, which enabled us to estimate the fraction of total PDE activity that was due to PDE4 [55]. This allowed us to compare both total PDE and PDE4-specific cAMP-hydrolyzing activity in the control subject and in the PDE4D-mutated patient 6 (Fig. 4). Surprisingly, we found that patient 6 exhibited total PDE and PDE4-specific activities that were similar to those of the control subject. This may be

Table 2
The average binding affinities of PDE4D WT and mutants (p.Gly673Asp and p.Ile678Thr). Standard deviations of the binding affinity shown in parenthesis were calculated based on 30 flexible docking simulations. The WT protein is slightly more stable with cAMP (by approximately 0.17 kcal/mol) than the 2 mutants. The number of successful bindings of cAMP to the binding pocket is 30 for WT protein and 4 and 9 for the 2 mutants.

Models	Average binding affinity (kcal/mol)	Number of successful binding of the 30 trials
WT	−8.70 (±0.000)	30
p.Gly673Asp (Pt 2)	−8.51 (±0.311)	4
p.Ile678Thr (Pt 1)	−8.56 (±0.292)	9

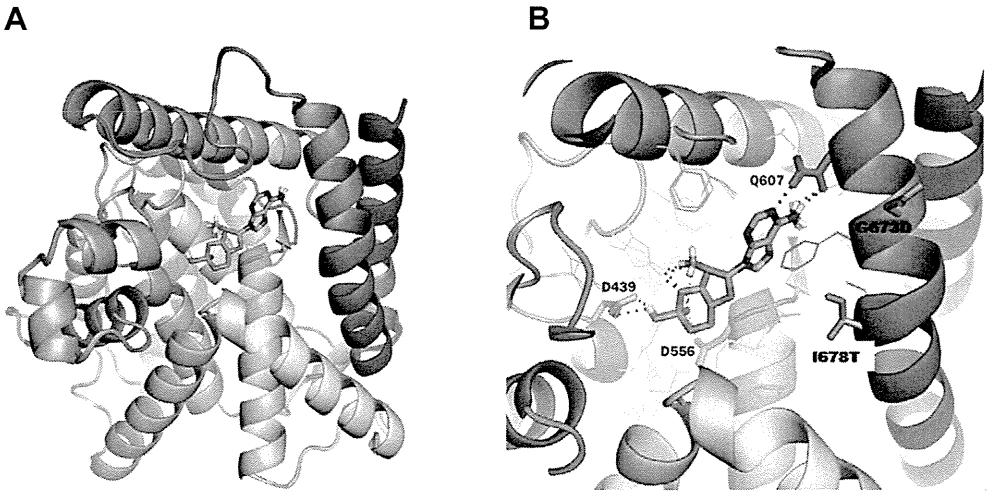

Fig. 2. Three dimensional structural models of the catalytic domain of PDE4D. Panel A shows the protein model of WT PDE4D with cAMP and panel B shows the models of the mutants (p.Gly673Asp and p.Ile678Thr) with cAMP. The 3 structures were superposed using the pyMOL program, and the cAMP ligand is positioned at the lowest-energy binding site found in the docking simulation. The binding between the protein and cAMP is shown in detail. D503, D620, and Q671 are known to be conserved binding residues. Side-chains of G673D and I678T are depicted by purple stick figures on the right-hand side of the binding pocket.

because PDE4D isoforms contribute little to the total PDE4 activity in these cells, or because in patient 6 the loss of PDE4D activity was compensated for by the up-regulation of catalytically functional PDE4 from other subfamilies.

3.5. Expression of PDE4 and its isoforms in patient cells

We sought to determine if the expression of PDE4 from other subfamilies was altered in patient 6, and we found a dramatic increase in PDE4C expression in the patient (Fig. 4D). By contrast, no changes were detected in the expression of PDE4A and PDE4B subfamilies (Fig. 4D). We also noted that *PDE4D5* and *PDE4D11* mRNA levels in the cells from patient 6 were double than that in control cells (Fig. 4D). This increase in transcripts correlated with an elevated PDE4D5 protein level relative to control, which was shown by staining by a PDE4D5-specific antibody (Fig. 4E).

Our expression-analysis data indicate that in patient 6, the loss of PDE4D activity was compensated for not only through the up-regulation of PDE4D5 and PDE4D11, which would be catalytically compromised, but also through the up-regulation of PDE4C. We propose that these changes help compensate for the reduced catalytic activity of PDE4D isoforms and could explain why total PDE4 activity was almost identical in the EBV-immortalized lymphocytes obtained from the control subject and patient 6 (Fig. 4, A–C).

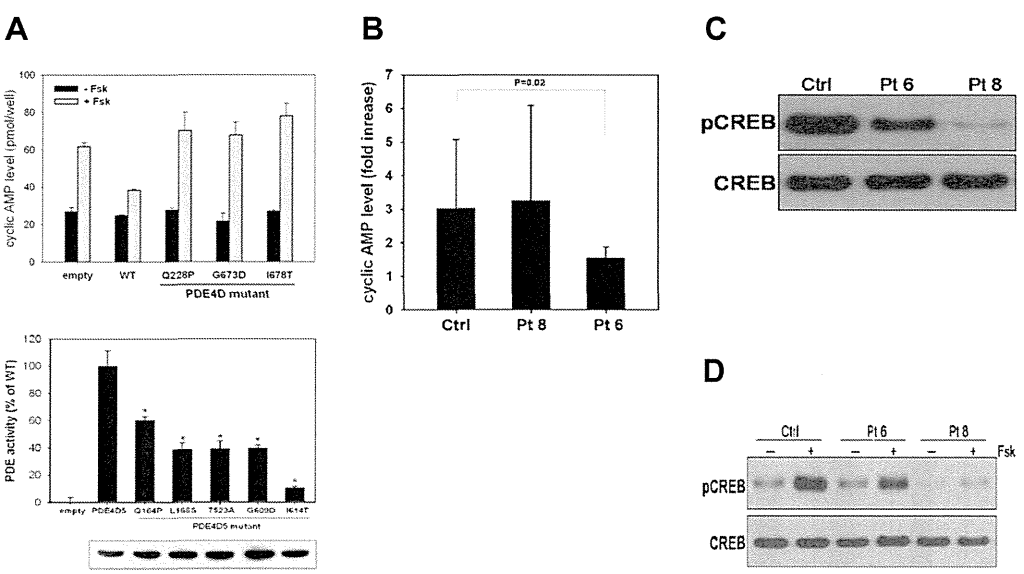

Fig. 3. Phosphorylation of cAMP responsive element-binding (CREB) protein in acrodysostosis patients. A. Functional studies on PDE4D in HEK 293 cells. Panel A shows measurement of cAMP in HEK293 cells transfected PDE4D5 WT and mutant constructs. Because the PDE4D isoform is the major species that has cAMP-hydrolyzing activity, we analyzed whether overexpressing recombinant WT or mutant PDE4D affects the cellular level of cAMP in HEK293 cells after treatment with the adenylyl-cyclase activator forskolin (Fsk, 10 μM). WT PDE4D decreased cellular cAMP levels, but overexpressed Q228P-, G673D-, and I678T-PDE4D mutants did not. Panel B shows the total PDE activity of PDE4D constructs. Compared to WT, all of PDE4D mutants had significantly reduced PDE activity. The results are shown as means ± SD. B. Levels of cAMP in EBV-transformed lymphocytes of control subject, patient 8, and patient 6 after treatment with forskolin (Fsk, 10 μM). In cells from patient 6 (with L230S mutation), cAMP levels showed a statistically significant decrease compared to control EBV-transformed lymphocytes. C. Phosphorylated CREB levels in control, patient 6, and patient 8 cells; both patients had lower than control pCREB levels. D. Diminished pCREB levels in patient cells were observed clearly after stimulating with Fsk for 30 min.

Table 3
PDE4D isoforms with mutation residue numbers.

PDE4D4	D1	D2	D3	D5	D6	D7	D8	D9	D10*	D11*
Type	Short	Short	Long	Long	Short	Long	Long	Long	Short	Short
Q228P	N/A	N/A	92	**164**	N/A	167	106	98	N/A	118
L230S	N/A	N/A	94	**166**	N/A	169	108	100	N/A	120
T587A	363	285	451	**523**	296	526	465	457	283	477
G673D	449	371	537	**609**	382	612	551	543	369	563
I678T	454	376	542	**614**	387	617	556	548	374	568

N/A — not applicable as mutation not in N-terminal portion of short form sequence. All clones are human except where indicated*, which are murine clones. The GenBank flat file numbers used are indicated in parentheses PDE4D1 (NP_001184151), PDE4D2, PDE4D3 (NP_006194), PDE4D4 (NP_001098101), PDE4D5 (NP_001184147), PDE4D6 (NP_001184152), PDE4D7 (NP_001159371), PDE4D8 (NP_001184148), PDE4D9 (NP_001184149), PDE4D10 (ABG57277) and PDE4D11 (ACA66114).

3.6. Immunofluorescent staining of EBV-transformed B cells

Immunofluorescence staining for PDE4D and the PDE4D scaffold proteins [7,22,56], RACK1 and β-arrestin, demonstrated similar colocalization in patient and control cells of PDE4D (Fig. 5).

3.7. PDE4D-KO rats

The role of *PDE4D* mutations in acrodysostosis was clarified by generating a PDE4D-KO rat. Body lengths measured at the ages of 3 and 5 weeks indicated significantly stunted growth in both male and female KO rats relative to WT rats (3 weeks: male to male, $P < 0.001$, female to female, $P < 0.001$; 5 weeks: male to male, $P < 0.001$, female to female, $P = 0.002$, Fig. 6A); stunted growth was observed in the KO and heterozygous rats compared to WT rats at 3 weeks ($P < 0.001$, Fig. 6B).

Skeletal radiographs of 10-week-old KO rats showed that the distal parts of the forelimbs (radius and palm) were shorter than in WT rats, and that all metacarpals and phalanges were shorter in KO rats than in WT rats (Fig. 6C and D).

4. Discussion

In this study, we have shown that *PDE4D* mutations are associated with acrodysostosis without apparent hormone resistance. The *PDE4D* gene encodes proteins that critically regulate Gsα-cAMP signaling by modulating the compartmentalization of this key signaling system through targeted cAMP degradation [7,19,57].

PDE4D-family enzymes hydrolyze cAMP and tightly regulate the Gsα-cAMP signal transduction pathway that employs PKA and Epac as its core effectors [7,54]. The *PDE4D* gene is associated with several distinct diseases or traits including ischemic stroke, neuroticism, asthma, and esophageal cancer [58–61]. Our work and 2 recently reported studies [62,63] implicate *PDE4D* as a third gene associated with Gsα-cAMP signaling-linked disorders; the others are *GNAS*, whose mutations are implicated in PHP-1a, pseudo-pseudohypoparathyroidism (PPHP), and progressive osseous heteroplasia (POH), and whose methylation defect is implicated in PHP-1b, and *PRKAR1A*, a nonsense mutation which is associated with acrodysostosis with hormone resistance [5,64].

From the clinical standpoint, our study and the 2 recent studies indicate that skeletal dysplasia may be causally related to hormonal resistance through a signal transduction pathway. At one end of hormonal resistance lies PHP-1b, which is manifested as a resistance to hormones like PTH and TSH. However, the skeletal manifestations associated with

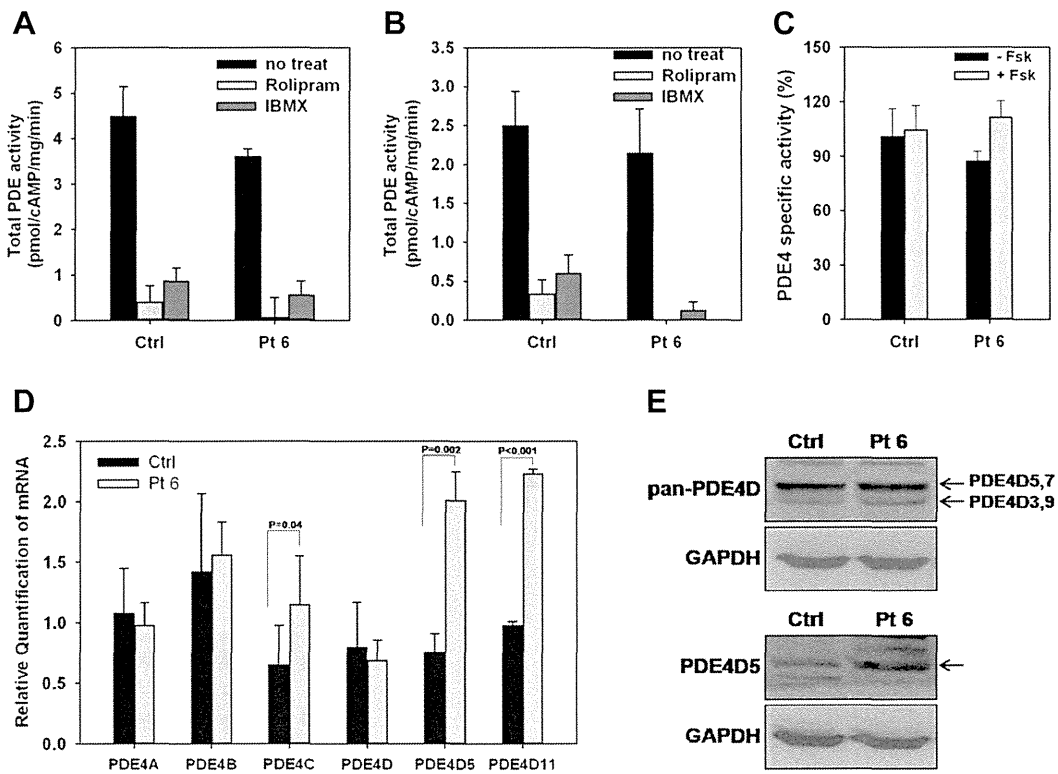

Fig. 4. Normal PDE4-specific activity in the acrodysostosis patient. EBV-transformed lymphocytes of control subject and patient 6 were harvested to measure the total PDE activity before (A) and after (B) Fsk stimulation (10 μM, 30 min) and also PDE4-specific activity (C). We measured the total cAMP-hydrolysing activity in the presence or absence of the pan-PDE inhibitor IBMX (100 μM), and in the presence of the PDE4-specific inhibitor rolipram (10 μM) to estimate the PDE4 fraction of the total PDE activity. In patient and control cells, total PDE and PDE4-specific activities were not different (means ± SD shown) (D). Because PDE4 activity levels were the same in the control subject and patient 6, we determined the expression of PDE4 and PDE4D isoform mRNAs in the patient. PDE4C isoform was increased in patient 6 in a statistically significant manner, and the expression of PDE4D isoforms was also increased; *$P < 0.05$, **$P < 0.005$ (E). PDE4D and PDE4D5 protein expressions. Overall PDE4D expression was similar in control and patient cells, but the expression of PDE4D5 isoform was slightly higher in patient cells.

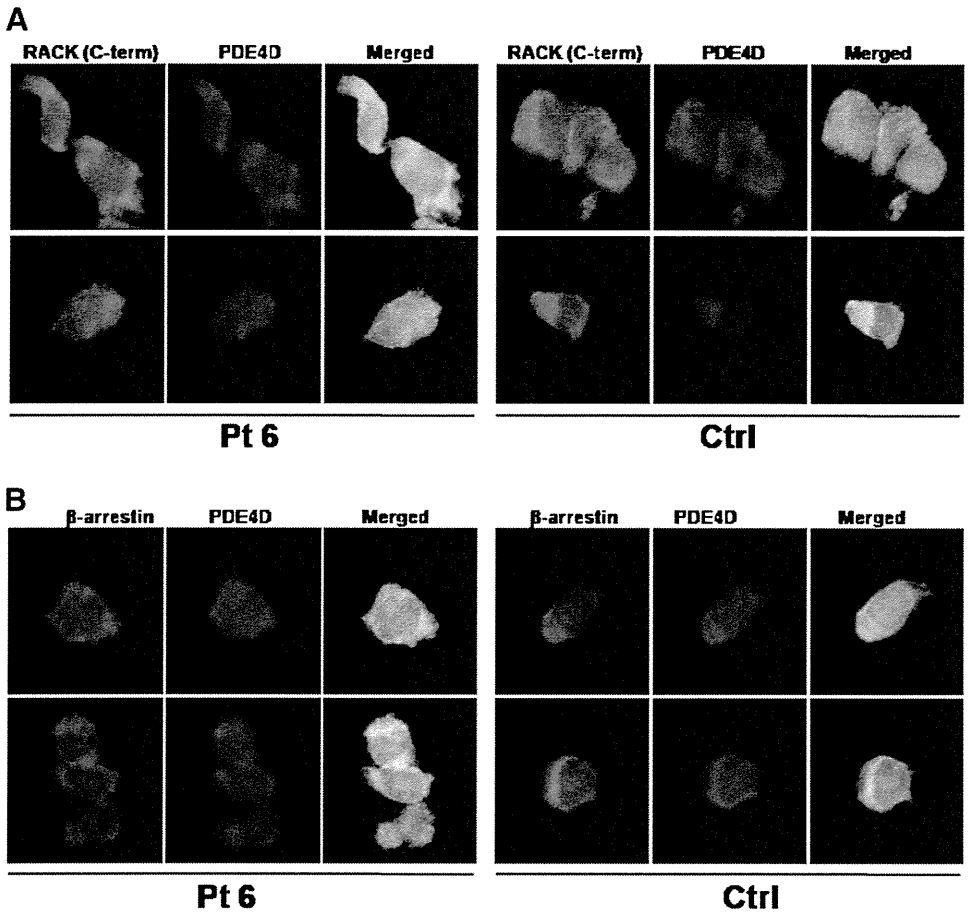

Fig. 5. Intracellular localization of PDE4D, RACK-1, and β-arrestin in EBV-transformed lymphocytes. Panel A shows the localization of PDE4D and RACK-1 in EBV-transformed lymphocytes. Immunofluorescent staining for RACK-1 and PDE4D were performed using rabbit anti-RACK-1 antibody and Alexa488-conjugated goat anti-rabbit IgG (left panel), and goat anti-PDE4D antibody and Alexa568-conjugated donkey anti-goat IgG (middle panel). Nuclei were counterstained with DAPI. Right panels show merged images of RACK-1 and PDE4D. Panel B shows the localization of PDE4D and β-arrestin in EBV-transformed lymphocytes. Immunofluorescent staining for beta-arrestin and PDE4D were performed using mouse anti-β-arrestin antibody and Alexa488-conjugated goat anti-mouse IgG (left panel), and goat anti-PDE4D antibody and Alexa568-conjugated donkey anti-goat IgG (middle panel). Nuclei were counterstained with DAPI. Right panels show merged images of β-arrestin and PDE4D. Colocalization of PDE4D and RACK-1 or β-arrestin was not different in cells from the patient and control subject.

PHP-1a (e.g., AHO) are accompanied by hormonal resistance. Remarkably, hormonal resistance is milder in patients with acrodysostosis caused by the *PRKAR1A* mutation, and even this hormonal resistance is apparently lost in acrodysostosis caused by *PDE4D* mutation. Therefore, hormonal resistance and skeletal dysplasia may represent a spectrum of signal transduction pathway-associated disorders, at least for AHO and acrodysostosis. We suggest that pursuing gene discovery in these diseases should continue, especially in patients who show combined mild hormonal resistance and skeletal manifestations.

In silico 3D structure analyses and in vitro transfection assays, using mutants that reflected those seen in the patients (Figs. 2 and 3), predicted an increase in the cAMP level caused by decreased PDE4D activity. However, our functional analyses of cells from patients with a PDE4D mutation were contradictory to this in that, compared to cells from control subjects, we observed a reduced, rather than an enhanced cAMP accumulation in response to forskolin activation of adenylyl cyclase. However, we resolved the basis of this apparent discrepancy by showing that, in cells from acrodysostosis patients, there appeared to be an up-regulation of PDE4 isoforms from other sub-families whose activity over-compensated for the loss of PDE4D activity (Fig. 4). Thus chronic adaptation to a deficient PDE4D environment appears to foster the over-compensation of the expression of other PDE4 species that likely explains the decreased cAMP accumulation and decreased CREB phosphorylation, compared to cells from normal subjects, seen in cells from acrodysostosis patients in response to forskolin challenge (Figs. 3 and 4). This parallels the situation where PKA activity is compromised by the *PRKAR1A* mutation, as in acrodysostosis without hormone resistance, which may explain why patients with inactivating PDE4D mutations phenotypically show acrodysostosis. Thus, it seems that acrodysostosis patients who are chronically expressing catalytically compromised PDE4D from conception elicits an adaptive response that takes the form of up-regulation of isoforms from other PDE4 subfamilies and that this overcompensates for the reduced activity caused by PDE4D mutation.

The myriad of 20+ PDE4 isoforms are believed to each have distinct, complex promoters but little, however, is known about their precise structure and regulation [65]. Nevertheless, previous studies on PDE4D5, PDE4A11, PDE4D1/2 has shown that they can confer both up- and down-regulation in response to altered cAMP levels [30–33, 66]. Thus analyses of the basis for the up-regulation of PDE4C, PDE4D5 and PDE4D11, which we observed in cells from acrodysostosis patients will require very considerable effort to resolve in future studies. Interestingly, however, there is a paucity of research that has been carried out on the PDE4C gene family and little is known about its precise functional significance, range of isoforms, regulation and distribution, except that it is poorly expressed in the brain [67,68]. However, we now know that an important consequence of PDE4 isoform diversity is that it allows the targeting of particular isoforms to specific signaling complexes,

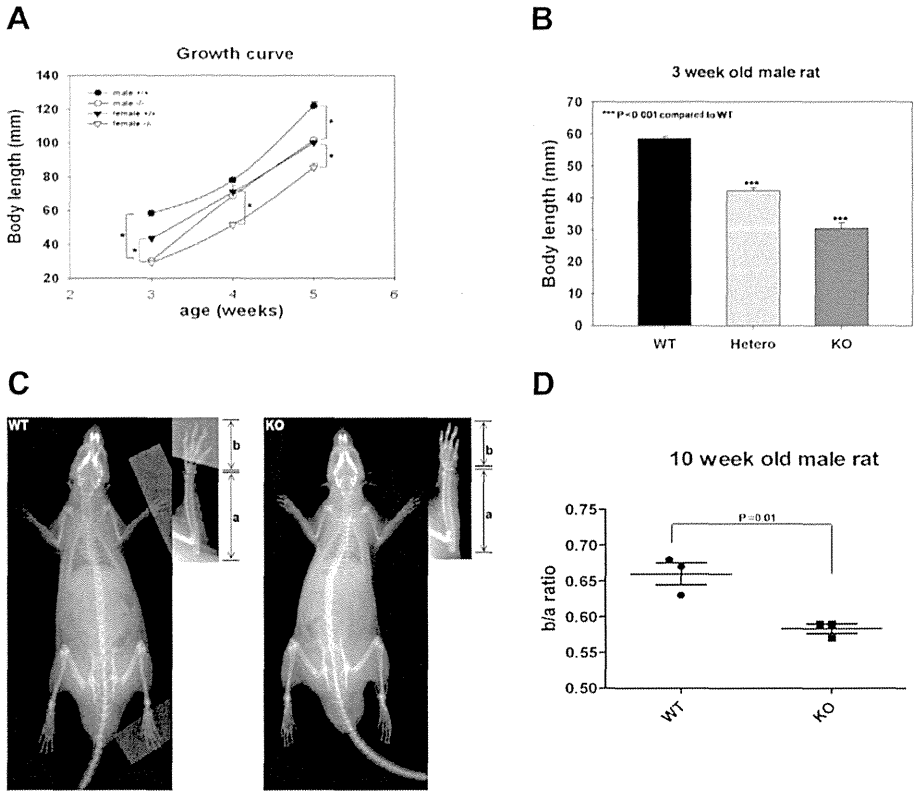

Fig. 6. Skeletal characteristics of PDE4D-KO rats. After birth, WT, heterozygous, and homozygous PDE4D-null rats were examined by measuring body length (nose-to-anus distance, N–A) using digital calipers. A. Starting from postnatal week 3, KO rats appeared significantly smaller than their control littermates. B. Male KO rats were significantly shorter than their WT and heterozygote littermates at 3 weeks. Data are shown as means ± SEM. C and D. The b/a ratios of male KO rats were significantly lower than those of WT rats at 10 weeks. Decreased b/a ratios correspond to brachydactyly, which is seen in patients with acrodysostosis. (a: length of a forearm; b: length of a forepaw).

which allows them to exert distinct functional roles [18]. Thus, while up-regulation of PDE4C may compensate for a lowering of overall PDE4 activity due to chronic expression of the mutant PDE4D isoforms, PDE4C is unlikely to result in identical sequestration of the same signaling complexes in cells that would be seen with the various PDE4D isoforms. This 'failure' is likely to elicit an up-regulation of PDE4C to higher levels than to be seen with PDE4D, as the cell strives to generate enough active PDE4 to pair with the signaling complexes involving PDE4D. Additionally, the mass action effect due to the increased level of PDE4 isoform expression in acrodysostosis with hormone resistance patients is likely to cause increased sequestration of binding partners involving PDE4C and PDE4D5/11, which may itself lead to functional changes [7].

The patients with *PDE4D* mutations notably had no apparent hormone resistance, unlike the patients with *PRKAR1A* mutations [5]. Our patient 3, who harbored the *PRKAR1A* mutation, as well as three patients with the same mutation in the previous report, had hormone resistance. However, our patients with *PDE4D* mutations did not show any clinical evidence of hormone resistance. One possible explanation for the presence or absence of hormone resistance in *PDE4D*-related acrodysostosis is related to the extreme diversity of the PDE isoenzymes and their tissue-specific patterns of expression. In fact, PDE4 is one of the main isoenzymes in the osteoblast [69]. On the other hand, *PRKAR1A* is a common pathway gene in the Gsα-cAMP-PKA signal transduction pathway; therefore, mutation in this gene may cause acrodysostosis as well as hormone resistance [70]. Another possibility is that if the core acrodysostosis phenotype in *PDE4D* mutation patients is due to compensatory up-regulation of PDE4C, with concomitant down-regulation of PKA activity and CREB phosphorylation, then the lack of hormone resistance may be due to the lowered PDE4D activity. This can be expected to allow activation of a pool of PKA sequestered close to it, as we have shown in 'dominant negative' approaches [21]. This would allow a key difference with *PRKAR1A* mutations, where all of the PKA-RI activity is compromised, to the *PDE4D* mutations where we propose that the major pool of PKA-RI activity will be compromised due to PDE4C up-regulation, while a PKA-RI pool associated with catalytically compromised PDE4D will be more active. Possibly, phosphorylation of a hormone receptor component associated with a PKA/PDE4D signaling complex negates hormone resistance in patients *PDE4D* mutations.

Finally, we tried to prove that loss of function of PDE4D in the long run results in the abnormalities of skeletal bone formation, as in human. In order to undertake this we employed a PDE4D knockout analysis using the rat, as mice are too small to discern the level of phenotypic change of KO expected. To address this hypothesis, we generated, for the first time, a KO of PDE4D in the rat; a larger rodent. In humans, skeletal manifestation of acrodysostosis without hormonal resistance consists of short stature, shortening of the distal part of the limb (especially the metacarpals and phalanges), and nasal bone hypoplasia. Nasal bone changes in the KO rat were difficult to discern. However, other manifestations in the bones were evident including significantly stunted growth in each gender at the age of 3 and 5 weeks. Moreover, this stunted growth was observed both in the KO rat and in heterozygote rats, as was it indeed noted in PDE4D deficient mice [71]. The most intriguing finding in this model was the observation that skeletal radiographs of 10-week-old KO rats showed shorter distal parts of the forelimbs (radius and palm) than in wild type rats and all of the metacarpals and phalanges of KO rat were also shorter than in the WT rat, as the name acrodysostosis implies. Our results show the strength of the KO rat model in terms of observing the relative bone change in the small bones.

It remains to be appreciated as to which specific PDE4D isoforms are critical to this pathology and whether mutations affect distinct isoform

differently. Certainly there is a growing appreciation that PDE4D isoforms perform distinct functional roles (see e.g. [21] and can provide important regulatory enzymes that affect cell proliferation [72]) and the cell cycle [73].

5. Conclusions

In conclusion, as has been observed with GNAS and PRKAR1A, PDE4D serves as a key regulatory element in the cAMP signal transduction pathway and influences bone formation that leads to skeletal dysplasia. We propose that specific inhibitory PDE4D mutations provide the focus that triggers the molecular pathology of acrodysostosis without hormone resistance. However, we need to appreciate that aspects of the pathological phenotype may well also be dependent on an over-compensatory induction of other PDE4 isoforms that can be expected to be targeted to different signaling complexes and exert distinct effects on compartmentalized cAMP signaling.

Conflict of interest

All of the authors have no conflict of interest.

Acknowledgments

This study was supported by grants from the Korea Healthcare Technology R&D Project, Ministry for Health, Welfare and Family Affairs, Republic of Korea (A080588), the Samsung Biomedical Research Institute grant (SBRI C-A9-240-3), the Korea Science and Engineering Foundation (KOSEF) grant funded by the Korean government (MEST) (no. 2008-006198), Center for Clinical Research (PHO 1100931 Green Cross), and a grant from the Ministry of Health, Labour and Welfare, Japan (H23-Jitsuyoka(Nanbyo)-Ippan-007). We thank KIAS Center for Advanced Computation for providing the Linux cluster system for computational modeling.

References

[1] L.C. Wilson, M.E. Oude Luttikhuis, M. Baraitser, H.M. Kingston, R.C. Trembath, J. Med. Genet. 34 (1997) 133–136.
[2] M.G. Butler, L.J. Rames, W.B. Wadlington, Am. J. Med. Genet. 30 (1988) 971–980.
[3] M.D. Houslay, G. Milligan, Trends Biochem. Sci. 22 (1997) 217–224.
[4] J.M. Graham Jr., D. Krakow, V.T. Tolo, A.K. Smith, R.S. Lachman, Pediatr. Radiol. 31 (2001) 2–9.
[5] A. Linglart, C. Menguy, A. Couvineau, C. Auzan, Y. Gunes, M. Cancel, E. Motte, G. Pinto, P. Chanson, P. Bougneres, E. Clauser, C. Silve, N. Engl. J. Med. 364 (2011) 2218–2226.
[6] M. Breckler, M. Berthouze, A.C. Laurent, B. Crozatier, E. Morel, F. Lezoualc'h, Cell. Signal. 23 (2011) 1257–1266.
[7] M.D. Houslay, Trends Biochem. Sci. 35 (2010) 91–100.
[8] C. Lugnier, Pharmacol. Ther. 109 (2006) 366–398.
[9] M.D. Houslay, P. Schafer, K.Y. Zhang, Drug Discov. Today 10 (2005) 1503–1519.
[10] C.P. Page, D. Spina, Curr. Opin. Pharmacol. 12 (2012) 275–286.
[11] C.P. Page, D. Spina, Handb. Exp. Pharmacol. (2011) 391–414.
[12] B. Beghe, K.F. Rabe, L.M. Fabbri, Am. J. Respir. Crit. Care Med. 188 (2013) 271–278.
[13] A. Hatzelmann, E.J. Morcillo, G. Lungarella, S. Adnot, S. Sanjar, R. Beume, C. Schudt, H. Tenor, Pulm. Pharmacol. Ther. 23 (2010) 235–256.
[14] K.F. Rabe, Br. J. Pharmacol. 163 (2011) 53–67.
[15] P.H. Schafer, R.M. Day, J. Am. Acad. Dermatol. 68 (2013) 1041–1042.
[16] M. Wittmann, P.S. Helliwell, Dermatol. Ther. (Heidelb) 3 (2013) 1–15.
[17] M. Conti, J. Beavo, Annu. Rev. Biochem. 76 (2007) 481–511.
[18] T. Keravis, C. Lugnier, Curr. Pharm. Des. 16 (2010) 1114–1125.
[19] M.D. Houslay, G.S. Baillie, D.H. Maurice, Circ. Res. 100 (2007) 950–966.
[20] K. McCormick, G.S. Baillie, Curr. Opin. Genet. Dev. 27C (2014) 20–25.
[21] A. McCahill, T. McSorley, E. Huston, E.V. Hill, M.J. Lynch, I. Gall, G. Keryer, B. Lygren, K. Tasken, G. van Heeke, M.D. Houslay, Cell. Signal. 17 (2005) 1158–1173.
[22] G.B. Bolger, G.S. Baillie, X. Li, M.J. Lynch, P. Herzyk, A. Mohamed, L.H. Mitchell, A. McCahill, C. Hundsrucker, E. Klussmann, D.R. Adams, M.D. Houslay, Biochem. J. 398 (2006) 23–36.
[23] G.S. Baillie, A. Sood, I. McPhee, I. Gall, S.J. Perry, R.J. Lefkowitz, M.D. Houslay, Proc. Natl. Acad. Sci. U. S. A. 100 (2003) 940–945.
[24] A. Terrin, S. Monterisi, A. Stangherlin, A. Zoccarato, A. Koschinski, N.C. Surdo, M. Mongillo, A. Sawa, N.E. Jordanides, J.C. Mountford, M. Zaccolo, J. Cell Biol. 198 (2012) 607–621.
[25] M.J. Lynch, G.S. Baillie, A. Mohamed, X. Li, C. Maisonneuve, E. Klussmann, G. van Heeke, M.D. Houslay, J. Biol. Chem. 280 (2005) 33178–33189.
[26] Y. Shakur, J.G. Pryde, M.D. Houslay, Biochem. J. 292 (Pt 3) (1993) 677–686.
[27] E. Huston, I. Gall, T.M. Houslay, M.D. Houslay, J. Cell Sci. 119 (2006) 3799–3810.
[28] G.S. Baillie, E. Huston, G. Scotland, M. Hodgkin, I. Gall, A.H. Peden, C. MacKenzie, E.S. Houslay, R. Currie, T.R. Pettitt, A.R. Walmsley, M.J. Wakelam, J. Warwicker, M.D. Houslay, J. Biol. Chem. 277 (2002) 28298–28309.
[29] M.J. Lynch, G.S. Baillie, M.D. Houslay, Biochem. Soc. Trans. 35 (2007) 938–941.
[30] E. Vicini, M. Conti, Mol. Endocrinol. 11 (1997) 839–850.
[31] I.R. Le Jeune, M. Shepherd, G. Van Heeke, M.D. Houslay, I.P. Hall, J. Biol. Chem. 277 (2002) 35980–35989.
[32] D.A. Wallace, L.A. Johnston, E. Huston, D. MacMaster, T.M. Houslay, Y.F. Cheung, L. Campbell, J.E. Millen, R.A. Smith, I. Gall, R.G. Knowles, M. Sullivan, M.D. Houslay, Mol. Pharmacol. 67 (2005) 1920–1934.
[33] A. McCahill, L. Campbell, T. McSorley, A. Sood, M.J. Lynch, X. Li, C. Yan, G.S. Baillie, M.D. Houslay, (PDE4A10), Cell. Signal. 20 (2008) 2071–2083.
[34] G. Bolger, T. Michaeli, T. Martins, T. St John, B. Steiner, L. Rodgers, M. Riggs, M. Wigler, K. Ferguson, Mol. Cell. Biol. 13 (1993) 6558–6571.
[35] C. Sette, M. Conti, J. Biol. Chem. 271 (1996) 16526–16534.
[36] N. Oki, S.I. Takahashi, H. Hidaka, M. Conti, J. Biol. Chem. 275 (2000) 10831–10837.
[37] D. Mika, W. Richter, R.E. Westenbroek, W.A. Catterall, M. Conti, J. Cell Sci. 127 (2014) 1033–1042.
[38] D. Willoughby, G.S. Baillie, M.J. Lynch, A. Ciruela, M.D. Houslay, D.M. Cooper, J. Biol. Chem. 282 (2007) 34235–34249.
[39] R. Hoffmann, I.R. Wilkinson, J.F. McCallum, P. Engels, M.D. Houslay, Biochem. J. 333 (Pt 1) (1998) 139–149.
[40] M.B. Beard, A.E. Olsen, R.E. Jones, S. Erdogan, M.D. Houslay, G.B. Bolger, J. Biol. Chem. 275 (2000) 10349–10358.
[41] S.J. MacKenzie, G.S. Baillie, I. McPhee, C. MacKenzie, R. Seamons, T. McSorley, J. Millen, M.B. Beard, G. van Heeke, M.D. Houslay, (UCR1), Br. J. Pharmacol. 136 (2002) 421–433.
[42] D.M. Collins, H. Murdoch, A.J. Dunlop, E. Charych, G.S. Baillie, Q. Wang, F.W. Herberg, N. Brandon, A. Prinz, M.D. Houslay, (PDE4D3) in a manner that is dynamically regulated through Protein Kinase A (PKA), Cell. Signal. 20 (2008) 2356–2369.
[43] K.F. MacKenzie, D.A. Wallace, E.V. Hill, D.F. Anthony, D.J. Henderson, D.M. Houslay, J. S. Arthur, G.S. Baillie, M.D. Houslay, Biochem. J. 435 (2011) 755–769.
[44] N. Niikawa, I. Matsuda, T. Ohsawa, T. Kajii, Hum. Genet. 42 (1978) 227–232.
[45] J.M. Ko, K.S. Kwack, S.-H. Kim, H.-J. Kim, J. Genet. Med. 7 (2010) 145–150.
[46] E. Nii, M. Urawa, T. Nshimura, H. Kitou, S. Ikegawa, S. Shimizu, H. Taneda, A. Uchida, N. Niikawa, Am. J. Med. Genet. B Neuropsychiatr. Genet. 144B (2007) 824–825.
[47] G.B. Bolger, S. Erdogan, R.E. Jones, K. Loughney, G. Scotland, R. Hoffmann, I. Wilkinson, C. Farrell, M.D. Houslay, Biochem. J. 328 (Pt 2) (1997) 539–548.
[48] K. Joo, J. Lee, S. Lee, J.H. Seo, S.J. Lee, J. Lee, Proteins 69 (Suppl. 8) (2007) 83–89.
[49] K. Joo, J. Lee, I. Kim, S.J. Lee, J. Lee, Biophys. J. 95 (2008) 4813–4819.
[50] K. Joo, J. Lee, J.H. Seo, K. Lee, B.G. Kim, J. Lee, Proteins 75 (2009) 1010–1023.
[51] M. Tress, J. Cheng, P. Baldi, K. Joo, J. Lee, J.H. Seo, J. Lee, D. Baker, D. Chivian, D. Kim, I. Ezkurdia, Proteins 69 (Suppl. 8) (2007) 137–151.
[52] O. Trott, A.J. Olson, J. Comput. Chem. 31 (2010) 455–461.
[53] B. Lu, A.M. Geurts, C. Poirier, D.C. Petit, W. Harrison, P.A. Overbeek, C.E. Bishop, Mamm. Genome 18 (2007) 338–346.
[54] G.S. Baillie, FEBS J. 276 (2009) 1790–1799.
[55] M.D. Houslay, D.R. Adams, Biochem. J. 370 (2003) 1–18.
[56] K.J. Smith, G.S. Baillie, E.I. Hyde, X. Li, T.M. Houslay, A. McCahill, A.J. Dunlop, G.B. Bolger, E. Klussmann, D.R. Adams, M.D. Houslay, Cell. Signal. 19 (2007) 2612–2624.
[57] H.V. Edwards, F. Christian, G.S. Baillie, Semin. Cell Dev. Biol. 23 (2012) 181–190.
[58] B.E. Himes, G.M. Hunninghake, J.W. Baurley, N.M. Rafaels, P. Sleiman, D.P. Strachan, J. B. Wilk, S.A. Willis-Owen, B. Klanderman, J. Lasky-Su, R. Lazarus, A.J. Murphy, M.E. Soto-Quiros, L. Avila, T. Beaty, R.A. Mathias, I. Ruczinski, K.C. Barnes, J.C. Celedon, W.O. Cookson, W.J. Gauderman, F.D. Gilliland, H. Hakonarson, C. Lange, M.F. Moffatt, G.T. O'Connor, B.A. Raby, E.K. Silverman, S.T. Weiss, Am. J. Hum. Genet. 84 (2009) 581–593.
[59] S. Shifman, A. Bhomra, S. Smiley, N.R. Wray, M.R. James, N.G. Martin, J.M. Hettema, S.S. An, M.C. Neale, E.J. van den Oord, K.S. Kendler, X. Chen, D.I. Boomsma, C.M. Middeldorp, J.J. Hottenga, P.E. Slagboom, J. Flint, Mol. Psychiatry 13 (2008) 302–312.
[60] S. Gretarsdottir, G. Thorleifsson, S.T. Reynisdottir, A. Manolescu, S. Jonsdottir, T. Jonsdottir, T. Gudmundsdottir, S.M. Bjarnadottir, O.B. Einarsson, H.M. Gudjonsdottir, M. Hawkins, G. Gudmundsson, H. Gudmundsdottir, H. Andrason, A.S. Gudmundsdottir, M. Sigurdardottir, T.T. Chou, J. Nahmias, S. Goss, S. Sveinbjornsdottir, E.M. Valdimarsson, F. Jakobsson, U. Agnarsson, V. Gudnason, G. Thorgeirsson, J. Fingerle, M. Gurney, D. Gudbjartsson, M.L. Frigge, A. Kong, K. Stefansson, J.R. Gulcher, Nat. Genet. 35 (2003) 131–138.
[61] C. Wu, Z. Hu, Z. He, W. Jia, F. Wang, Y. Zhou, Z. Liu, Q. Zhan, Y. Liu, D. Yu, K. Zhai, J. Chang, Y. Qiao, G. Jin, Z. Liu, Y. Shen, C. Guo, J. Fu, X. Miao, W. Tan, H. Shen, Y. Ke, Y. Zeng, T. Wu, D. Lin, Nat. Genet. 43 (2011) 679–684.
[62] C. Michot, C. Le Goff, A. Goldenberg, A. Abhyankar, C. Klein, E. Kinning, A.M. Guerrot, P. Flahaut, A. Duncombe, G. Baujat, S. Lyonnet, C. Thalassinos, P. Nitschke, J.L. Casanova, M. Le Merrer, A. Munnich, V. Cormier-Daire, Am. J. Hum. Genet. 90 (2012) 740–745.
[63] H. Lee, J.M. Graham Jr., D.L. Rimoin, R.S. Lachman, P. Krejci, S.W. Tompson, S.F. Nelson, D. Krakow, D.H. Cohn, Am. J. Hum. Genet. 90 (2012) 746–751.
[64] L.S. Kirschner, J.A. Carney, S.D. Pack, S.E. Taymans, C. Giatzakis, Y.S. Cho, Y.S. Cho-Chung, C.A. Stratakis, Nat. Genet. 26 (2000) 89–92.
[65] M.D. Houslay, Prog. Nucleic Acid Res. Mol. Biol. 69 (2001) 249–315.

[66] G. Rena, F. Begg, A. Ross, C. MacKenzie, I. McPhee, L. Campbell, E. Huston, M. Sullivan, M.D. Houslay, Mol. Pharmacol. 59 (2001) 996–1011.
[67] M. Sullivan, A.S. Olsen, M.D. Houslay, Cell. Signal. 11 (1999) 735–742.
[68] R.J. Owens, S. Lumb, K. Rees-Milton, A. Russell, D. Baldock, V. Lang, T. Crabbe, M. Ballesteros, M.J. Perry, Cell. Signal. 9 (1997) 575–585.
[69] S. Wakabayashi, T. Tsutsumimoto, S. Kawasaki, T. Kinoshita, H. Horiuchi, K. Takaoka, J. Bone Miner. Res. 17 (2002) 249–256.
[70] S.R. Neves, P.T. Ram, R. Iyengar, Science 296 (2002) 1636–1639.
[71] S.L. Jin, F.J. Richard, W.P. Kuo, A.J. D'Ercole, M. Conti, Proc. Natl. Acad. Sci. U. S. A. 96 (1999) 11998–12003.
[72] D.J. Henderson, A. Byrne, K. Dulla, G. Jenster, R. Hoffmann, G.S. Baillie, M.D. Houslay, Br. J. Cancer 110 (2014) 1278–1287.
[73] C.L. Sheppard, L.C. Lee, E.V. Hill, D.J. Henderson, D.F. Anthony, D.M. Houslay, K.C. Yalla, L.S. Cairns, A.J. Dunlop, G.S. Baillie, E. Huston, M.D. Houslay, Cell. Signal. 26 (2014) 1958–1974.

Pediatric Neurology 50 (2014) 31–37

Contents lists available at ScienceDirect

Pediatric Neurology

journal homepage: www.elsevier.com/locate/pnu

Original Article

Corticosteroid Therapy for Duchenne Muscular Dystrophy: Improvement of Psychomotor Function

Yuko Sato PhD [a,b], Akemi Yamauchi MD, PhD [b], Mari Urano MA [b], Eri Kondo MD [b], Kayoko Saito MD, PhD [a,b,*]

[a] *Affiliated Field of Genetic Medicine, Division of Biomedical Engineering and Science, Graduate Course of Medicine, Graduate School of Tokyo Women's Medical University, Tokyo, Japan*
[b] *Institute of Medical Genetics, Tokyo Women's Medical University, Tokyo, Japan*

ABSTRACT

BACKGROUND: Of the numerous clinical trials for Duchenne muscular dystrophy, only the corticosteroid prednisolone has shown potential for temporal improvement in motor ability. In this study, the effects of prednisolone on intellectual ability are examined in 29 cases of Duchenne muscular dystrophy because little information has been reported. And also, motor functions and cardiac functions were evaluated. **METHODS:** The treated group was administered prednisolone (0.75 mg/kg) orally on alternate days and the compared with the untreated control group. Gene mutations were investigated. The patients were examined for intelligence quotient adequate for age, brain natriuretic peptide, creatine kinase, and manual muscle testing before treatment and after the period 6 months to 2 years. **RESULTS:** Intelligence quotient scores of the treated increased to 6.5 ± 11.9 (mean ± standard deviation) were compared with the controls 2.1 ± 4.9 ($P = 0.009$). Intelligence quotient scores of the patients with nonsense point mutations improved significantly (21.0 ± 7.9) more than those with deletion or duplication (1.9 ± 9.0; $P = 0.015$). Motor function, such as time to stand up, of those treated improved significantly and brain natriuretic peptide level was reduced to a normal level after treatment in 15 patients (73%). **CONCLUSIONS:** Our results demonstrate the effectiveness of prednisolone in improving intellectual impairment as well as in preserving motor function and brain natriuretic peptide levels. We presume that prednisolone has a read-through effect on the stop codons in the central nervous systems of Duchenne muscular dystrophy because intelligence quotient of point mutation case was improved significantly.

Keywords: Duchenne muscular dystrophy, prednisolone, cognition, motor function

Pediatr Neurol 2014; 50: 31-37

Introduction

Duchenne muscular dystrophy (DMD) is the most common type of childhood muscular dystrophy. It is characterized by progressive muscle weakness and deterioration of skeletal and cardiac muscle function. DMD is an X-linked recessive disorder, caused by mutations in the *DMD* gene in Xp21.1, leading to complete absence of the cytoskeletal protein dystrophin in both skeletal and cardiac muscle cells.[1] Several treatments involving drugs with read-through effects have attracted major interest, such as the amino glycoside antibiotic gentamicin[2,3] and PTC124[4] as well as antisense morpholinos that cause exon skipping.[5] These treatments are, however, being administered only as clinical research regimens at present and have not yet reached the stage of extensive clinical application. The only widely used clinically effective treatment for DMD patients is oral administration of prednisolone (PSL). This treatment was highly evaluated, as evidence level 1, by the US Neurology Academy and at the US Pediatric Neurology Meeting in 2005.[6]

PSL is believed to temporarily slow motor function decline and disease progression. In our daily examination of

Article History:
Received March 20, 2013; Accepted in final form July 31, 2013

* Communications should be addressed to: Dr. Saito; Director and Professor, Institute of Medical Genetics; Tokyo Women's Medical University; 10-22 kawada-cho; shinjyuku-ku; Tokyo 162-0054, Japan.
E-mail address: saito@img.twmu.ac.jp

0887-8994/$ - see front matter © 2014 Elsevier Inc. All rights reserved.
http://dx.doi.org/10.1016/j.pediatrneurol.2013.07.022